Environmental Science and Pollution Research
https://doi.org/10.1007/s11356-023-30093-8

A critical review on graphene and graphene-based derivatives from natural sources emphasizing on CO_2 adsorption potential

Saswata Chakraborty[1] · Ranadip Saha[1] · Sudeshna Saha[1]

Received: 17 July 2023 / Accepted: 22 September 2023
© The Author(s), under exclusive licence to Springer-Verlag GmbH Germany, part of Springer Nature 2023

Abstract
Accelerated release of carbon dioxide (CO_2) into the atmosphere has become a critical environmental issue, and therefore, efficient methods for capturing CO_2 are in high demand. Graphene and graphene-based derivatives have demonstrated promising potential as adsorbents due to their unique properties. This review aims to provide an overview of the latest research on graphene and its derivatives fabricated from natural sources which have been utilized and may be explored for CO_2 adsorption. The necessity of this review lies in the need to explore alternative, sustainable sources of graphene that can contribute to the development of viable environmentally benign CO_2 capture technologies. The review will aim to highlight graphene as an excellent CO_2 adsorbent and the possible avenues, advantages, and limitations of the processes involved in fabricating graphene and its derivatives sourced from both industrial resources and organic waste-based naturally occurring carbon precursors for CO_2 adsorption. This review will also highlight the CO_2 adsorption mechanisms focusing on density functional theory (DFT) and molecular dynamics (MD)–based studies over the last decade.

Keywords Graphene · Graphene-based derivatives · CO_2 adsorption · Solid sorbents · Graphene from natural resources · Graphene from industrial sources · CO_2 capture mechanism · DFT analysis

Introduction

Since the inception of the industrial revolution, there has been a reliance on fossil fuels, which causes substantial amounts of carbon dioxide released into the atmosphere every second. With the progression of time, there has been an expansion of industrialization on a global scale, advances in technology such as genetically modified crops, and improved medicine, and greater distribution of such advancements across the entire globe due to improved connectivity and globalization has led to a population boom (The human population has amplified from two billion in 1930 to 7 billion in 2011. The human population currently stands at 8 billion at the end of 2022.). This has resulted in even greater quantities of carbon dioxide being released into the environment due to human civilization footprint (Fig. 1). The quantity of carbon dioxide being added to the atmosphere has displayed an exponential increase from 2010 to 2022, with a combined CO_2 emission greater than that of all the years of the post-industrial revolution till 2009. In the year 1927, the total carbon dioxide emission from the burning of fossil fuels and industry was at 3.9 billion tons per year, while it was 31.51 billion tons at the end of 2006. Currently, it has escalated to 37.2 billion tons in 2021, with a projected growth of 1% for the year 2022. The current daily average reading for atmospheric CO_2 on the planet is 417.46 ppm (parts per million), at Mauna Loa Observatory, Hawaii. This constant release of carbon dioxide has resulted in global warming (carbon dioxide resulting from the burning of fossil fuels contributes to nearly 60% of global warming), the phenomenon in which the average temperature of the Earth's atmosphere rises due to the presence of greenhouse gases which prevent the incident solar radiation from being reflected by the earth back into space. With increasing carbon dioxide concentration in the atmosphere, the global surface temperature of the earth has ascended by 1.1–1.8 °C more than the

Responsible Editor: Tito Roberto Cadaval Jr

✉ Sudeshna Saha
sudeshna.saha@jadavpuruniversity.in

[1] Chemical Engineering Department, Jadavpur University, 188, Raja S. C. Mullick Road, Kolkata 700032, India

Published online: 02 October 2023

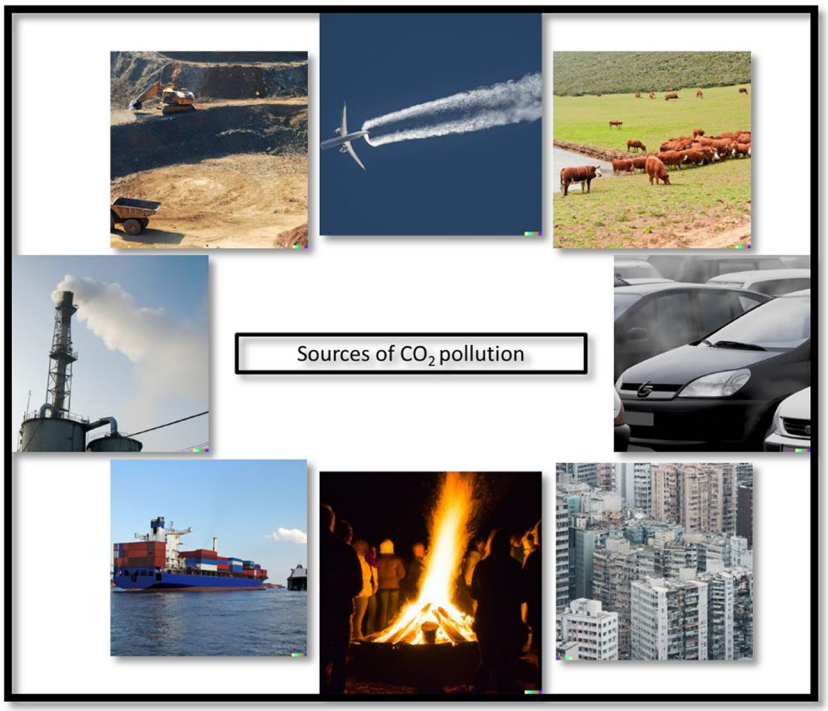

Fig. 1 Sources of carbon dioxide emission to the environment

nineteenth and twentieth century average. Since 1981, the rate of warming has doubled per decade (0.18 °C per decade). In 2022 earth's surface temperature was 0.86 °C higher compared to the twentieth-century average of 13.9 °C and 1.06 °C higher than the pre-industrial period (1880–1900). This has resulted in the global average temperature rise of 1 °C in comparison to the pre-industrial period (1880–1900). The heat capacity of the earth is massive, considering the tremendous size and capacity of the oceans. This one-degree increase has resulted in extreme amounts of accumulated heat leading to seasonal temperature extremes, reduction of snow cover, increase in the amount of heavy rainfall, and noticeable change in the habitat of all living beings. The average increase in land and ocean temperature was 0.08 °C per decade from 1880; however, since 1981, the temperature increase rate has more than doubled to 0.18 °C per decade. The last decade (2014–2022) has witnessed the hottest 9 years in a row with the 10 warmest years on record having all occurred since 2010. Unless greenhouse gas emissions are restricted, climate models predict that global surface temperature will increase by an additional 4 °C during the twenty-first century. Predictions regarding the effect on climate range from, speeding up of the water cycle leading to increased precipitation by 7% with each degree rise in temperature (distribution will be uneven throughout the planet), a greater quantity of snow and ice will melt as compared to the precipitation during the winter causing a gradual reduction in the ice caps with the Arctic facing a greater reduction than the Antarctic (collapse of major ice caps in Greenland and Antarctica). By 2050, the global sea levels will rise by an additional 0.25 to 0.30 m, reaching 1.1 m by the end of 2100. Oceans that act as a buffer for absorbing CO_2 will increase in pH (0.14 to 0.35), wreaking havoc on marine life; there will also be noticeable changes in ocean currents, severe weather, and cloud patterns, and disruption of thermohaline circulation. Studies reveal a possibility of a sudden release of methane gas trapped in the form of permafrost in the poles, endangering the livelihood of the whole planet. Initiatives, programs, conferences, and discussions on a global scale involving most nations across the globe have been undertaken to restrict the addition of carbon dioxide to the atmosphere, to reduce global warming and decelerate climate change, and various decisions have resulted from them. Stockholm hosted the first UN environmental conference in 1972. The agenda, which focused on concerns like chemical pollution, atomic bomb testing, and whaling, scarcely mentioned climate change. As a result, UN Environment Programme (UNEP) was created. The 1987 Montreal Protocol put restrictions on substances that harm the ozone layer. Despite not having been created with climate change in mind, it had a greater influence on greenhouse gas emissions than the Kyoto Protocol. The Intergovernmental Panel on Climate Change (IPCC) was founded in 1988 to bring together and evaluate climate change research. The IPCC released its First Assessment Report in 1990. It concluded that the increase in temperature by 0.3 to 0.6 °C during the past century was due to the increase in human emissions leading to an increased amount of greenhouse

gases in the atmosphere. Governments ratified the United Framework Convention on Climate Change in 1992 during the Rio de Janeiro Earth Summit. Its main goal was "stabilization of atmospheric greenhouse gas occurrence at a point that would avoid harmful human intervention with the climate system." Developed nations have consented unanimously to restrict their emissions to a level that was in 1990. The IPCC's Second Assessment Report, published in 1995, indicated "a discernible human effect" on climate change. This has been referred to as the first unambiguous admission that people are the main cause of accelerating climate change. Kyoto Protocol was approved in 1997. From 2008 to 2012, developed countries agreed to cut emissions by an average of 5%, with widely divergent national targets. According to the IPCC's Third Assessment Report issued in 2001, there was "new and stronger evidence" that greenhouse gas emissions from human activity are the primary reasons for the warming that transpired in the second half of the twentieth century. For those nations who are still party to it, the Kyoto Protocol became international law in 2005. In 2006, The Stern Review resolved that if left unchecked, climate change might reduce world GDP by up to 20%; however, reducing it would result in around 1% of global GDP. In 2007, the IPCC's Fourth Assessment Report concluded a greater than 90% chance that greenhouse gas emissions from human activity were the main reason for the current state of the climate. Scientists are 95% positive that humans are the "primary cause" of global warming since the 1950s, according to the first section of the IPCC's fifth assessment report in 2013. The Paris Agreement soon followed a landmark in the fight against climate change, embraced by 196 countries at COP21 in Paris on December 12, 2015, and implemented on November 4, 2016. The decision was taken to withhold global warming below 2 °C compared to the pre-industrial era. The main goal of this agreement is to reach the global peak of greenhouse gas emissions as soon as possible. One of the quantitative targets of this arrangement would be the establishment of zero-carbon discharge for the segments representing 70% of global emissions by 2030, to achieve a climate-neutral world by the mid-century period circa 2050. Fossil fuels will still be the major provider of energy (80%) in 2035, which will hinder the fulfillment of this objective. The additional route that may be undertaken to achieve the same goal would be the direct removal of carbon dioxide (CO_2) from the atmosphere.

The first carbon capture plant was proposed in 1938 and became functional in 1972, and the first integrated capture and storage system was set up in Norway in 1996. There are over 43 large-scale setups that are slowly chipping away at the current CO_2 stock in the atmosphere. Carbon capture for industrially produced CO_2 comprises the following routes: the post-combustion method, the oxyfuel process, and the pre-combustion process (Markewitz et al. 2012; Wilberforce et al. 2019).

The post-combustion process involves washing the flue gas with chemical solvents to absorb CO_2 from effluent streams from various industries. These solvents may be based on amines, ammonia, alkali, amino acid salt, aqueous carbonate, or even chilled ammonia (Fauth et al. 2012). Among the solvents MEA (methanol amine)-based liquid solvents are the most popular; however, the absorption has to be carried out at 40–60 °C, for which low-pressure steam has to be diverted from the electricity generation. As a result, an efficiency loss of 10 to 14% can occur (Nwaoha et al. 2017). Also, CO_2 in the flue gas must have a partial pressure of 3–15 kPa to achieve a degree of separation of 80–95%. A few set-ups are already in operation with a plant in Oklahoma, USA (with a daily production of 20 MW and CO_2 exhaust of 800 t CO_2/day), which can capture 15% of the released CO_2 (Kárászová et al. 2020). The plant in Sleipner, Norway, manages to capture over 1 million tons of CO_2 per year. This method however has certain drawbacks, the main problem being the decomposition of solvents in air. This is mainly because SO_x and $NO_x > 10$ ppm will cause the salt formation of amines which will require a high temperature to precipitate out (IPCC, 2005). The energy expenditure on CO_2 capture in this route varies around 4 GJ per ton of CO_2 captured, a setup in Esbjerg (Denmark) with a 30% MEA solvent requiring 3.7 GJ per ton of CO_2 captured, while similar energy requirements are required for the plant in NiederauBem (Germany) which manages to capture 7.2 t of CO_2 per day. Most upcoming and development power plants utilizing this technology have a restricted power output of less than 10 MW. Another innovation along this route has been the carbon looping method (calcium carbonate formed by carbonization of CaO at 600–700 °C followed by calcination at 900 °C). The efficiency loss of the power plant due to carbon capture modification has been less than 7.2%. In the most optimistic scenario, the efficiency loss of the plant due to the implementation of carbon capture technology will be 9.1% at the minimum (Scholes et al. 2020). The next process involves combustion in pure oxygen, which is named the *Oxyfuel process*; the key difference between conventional power plants and the post-combustion process is the composition of the flue gas, which has a CO_2 composition of 89% volume for the oxyfuel process while only being 12–15% by volume in the post-combustion process (Markewitz et al. 2012). Here, O_2, obtained from the air by cryogenic air separation units, is mixed with the fuel before combustion (Nemitallah et al. 2017). The current stoichiometric requirement of O_2 for combustion in power plants is about 1.15 times the fuel, which is about 270,000 m^3/h for a 500 MW plant; however, if the oxyfuel process is to be implemented, the required O_2 would be 800,000 m^3/h.

The temperatures attained in such a set-up would also be higher, which will pose a threat of mechanical damage to the unit (Nikolopoulos et al. 2011; Wu et al. 2019). This would require a portion of the flue gas to be returned with the feed stream. If an excess amount of O_2 required is compromised, burnout and corrosion can occur. Air-separation of O_2, with a purity demand of 99.5% for the process, has a very high energy requirement; a lower degree of purity causes a rise in energy requirements downstream. Also, excess residual oxygen is available after combustion, and although the volume of the flue gas generated is low, NO_x concentrations remain higher than accepted emission standards of coal-based power plants (365 ppm). A pilot plant setup in Germany of 30 MW capacity, utilizing the oxyfuel route, had to be fitted with denitrification units as the NO_x formation exceeded emission norms. On completing 1200 operating hours, 1000 tons of 99.7% pure CO_2 was captured with 90% carbon capture efficiency. An efficiency loss of 8–10% (6% loss from air separation unit, 7% from conventional cryogenic technology, and capture and processing of CO_2 intended for transport costing 3% efficiency) is observed. Some improvements which are currently being explored are the utilization of a high temperature-air separation membrane, permeable to O_2 only above a certain temperature, where adequate membrane material of sufficient mechanical strength has yet to be identified; another method would be chemical looping, where the fuel is oxidized by the metal oxide instead of molecular oxygen (which is then regenerated separately); this route prevents exposure of N_2 to high temperature; the utilization of mixed ion–electron conducting membrane can reduce efficiency loss to 8% (Nemitallah et al. 2017). The final process, the pre-combustion process, involves the decarbonization of the combustion gas. This is achieved by the gasification of fuels to synthesis gas, by the CO-shift reaction. CO_2 is captured using solvents before combustion from pressurized H_2-enriched flue gas obtained after CO-shift, i.e., air separation unit placed before the gasification process. The fuel gas obtained through this process exclusively consists of CO_2 and H_2. Only 5 integrated gasification combined cycle (IGCC) power plants without CO_2 capture have been fabricated across the world (2000), due to less credibility compared to conventional power plants (IPCC, 2005; Markewitz et al. 2012; Wilberforce et al. 2019; Olabi et al. 2022).

The implementation of carbon capture systems to reduce the global warming potential of conventional power plants has shown a noticeable effect, but the benefits are mostly of a reactive nature; these set-ups are reducing the carbon dioxide output of power plants, and the effects have been wide-ranging. They must not be restricted to capturing CO_2 from effluent streams, but also be able to actively capture CO_2 directly from the air thereby becoming effective at dealing with CO_2 from anthropogenic activities ranging from respiration to CO_2 developed due to intercontinental flights. The CO_2 capture capacity has to be improved to reduce efficiency losses which show up when carbon capture setups are introduced to any system. Presently, 18 direct air capture plants are in operation worldwide, chipping away almost 0.01 metric tons of CO_2 per year. Direct Air Capture Technology (DAC) includes both solid-sorbent–based systems and liquid-sorbent–based technologies. However, DAC is currently prohibitively expensive due to the excessive price of energy. Arguments for using reforestation to capture CO_2 fall short due to the space requirement of plantations, with the scarcity of available space and the extensive time requirement to grow complete forest patches, and DAC can do the same with 99.7% less space.

Graphene as a CO_2 capture material

Among solid sorbent–based systems, the nanomaterial graphene, a two-dimensional allotrope of carbon that is formed primarily of sp^2 hybridized carbon atoms (Fig. 2) (Armano and Agnello 2019), may be used as a molecular sieve to capture CO_2 (Chuah et al. 2021; Sun et al. 2021). Nanographene layers (NGL) with etched holes and defects are efficient at CO_2 capture (Huang et al. 2020). The cost requirements of graphene-based air adsorbents obtained from industrially sourced raw materials are very high, while the throughput of graphene obtained from naturally occurring carbon precursors is limited. Apart from pure graphene, reduced graphene oxide (RGO) may also be utilized as a CO_2 capture material. In terms of the quantity of material that can be created, graphene oxide (GO), an intermediary produced in the process of producing graphene, is easier to get than

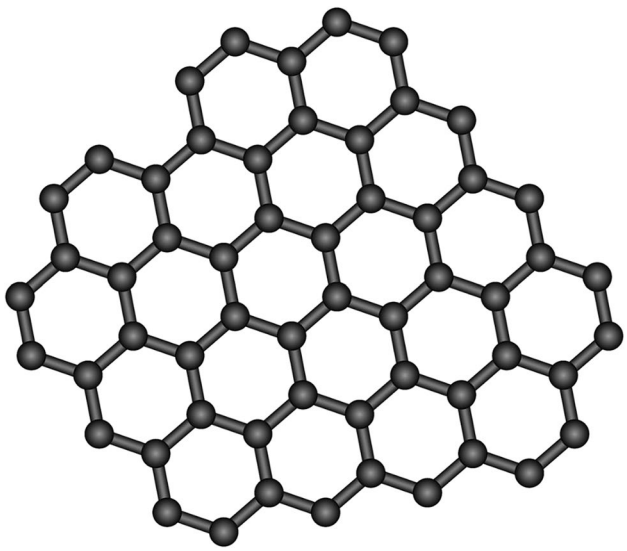

Fig. 2 Two-dimensional structure of graphene

pure graphene. RGO is also competitive with graphene in terms of CO_2 adsorption performance due to the presence of greater defects in the structure. The functionalization of graphene and derivatives of graphene improves its CO_2 adsorption ability (Fraga et al. 2019; Malekian et al. 2019). Mechanisms of graphene and GO formation are sensitive to process parameters and the choice of raw materials. Characterization techniques such as FTIR, SEM, TEM, BET, XPS, XRD, AFM, and Raman spectroscopy may be used to characterize graphene, RGO, their derivatives, and functionalized variants. The list of carbon sources for graphene and RGO is wide-ranging, with varying results in terms of CO_2 capture performance in the final product (Tarcan et al. 2020; Jiříčková et al. 2022). The most common source material for obtaining graphene via the top-down route is industrial-grade graphite, which is chemically exfoliated by the modified Hummer's method (Hummers and Offeman 1958) to obtain GO, which may be reduced to NGL or RGO. The bottom-up route involves the use of naturally available carbon sources, which are first carbonized and then graphitized utilizing chemical exfoliation (Viculis et al. 2003), catalytic oxidation (Lin et al. 2013), thermal treatments (Chowdhury and Balasubramanian 2016), and chemical treatments to yield graphene and RGO. More advanced methods for obtaining etched NGL involve bombarding the NGL with ozone in specialized reactors (Hsu et al. 2021), chemical vapor deposition (CVD) of high-quality graphene directly onto a template (Fujita et al. 2017), and the use of coordination compounds like ferrocene to treat carbonized precursors with ongoing thermal treatment to obtain GO (Zhao and Zhao 2013; Hashmi et al. 2020; Tamilselvi et al. 2020). As per the Web of Science Database, as of July 2023, there have been over 150,000 research papers published on graphene, over 10,000 research papers published on graphene-based adsorbent for CO_2 capture. However, the number of papers that investigate graphene sourced from natural and waste-based carbon precursors as CO_2 adsorbents only ranges in the hundreds. A similar scenario is observed from data obtained from the dimensions metric where the papers which investigate graphene sourced from natural and waste-based carbon precursors as CO_2 adsorbents dramatically reduce the actual quantity of research work carried out on graphene as shown in the graph (Fig. 3). Graphene obtained from graphite and other industrial-grade sources limits graphene to be used as a CO_2 adsorbent on a large scale due to the inhibitory costs of high-grade graphite and the chemicals involved in Hummer's method. In the last few years, between 2014 and 2022, there has been a 200% growth in the number of publications related to graphene fabrication from natural carbon resources emphasizing environmentally benign routes of graphene preparation.

The objective of the review would be to categorize and identify graphene and GO derivatives based on the carbon precursor, the synthesis route, the process parameters, and the CO_2 capture performance. Although a lot of interesting and insightful review papers have been published in the last decade on CO_2 capture by graphene and graphene derivatives (Lee and Park 2012; Tarcan et al. 2020; Bermeo et al. 2022; Castro-Muñoz et al. 2022; Gao et al. 2022; Gunawardene et al. 2022; Ramar and Balraj 2022; Wei et al. 2022; Zhu et al. 2022), this review will focus on graphene and its derivatives fabricated from natural and waste carbon sources, their properties, and specific possible uses for CO_2 adsorption. Graphene from natural resources is still at its primitive stage of research as inferred from the number of publications; this review will give an insight into the efficacy of the processes involved in the fabrication of graphene from natural resources, the drawbacks of the processes involved, and a pathway to overcome the limitations.

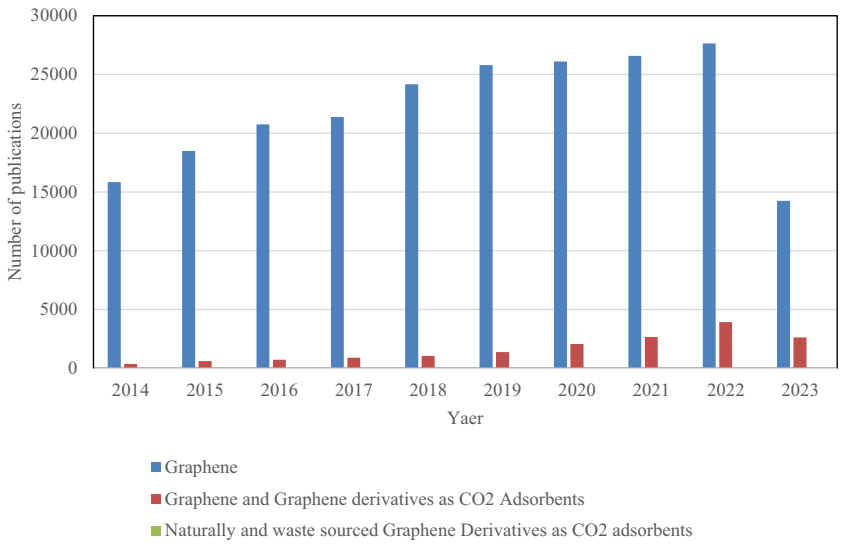

Fig. 3 Year-wise publication of graphene and its derivatives for the last decade

Mechanism of CO_2 capture by graphene

The CO_2 capture mechanism is dictated by the chemical and physical characteristics of the adsorbent material. It has been observed that graphene can adsorb CO_2 by both physisorption and chemisorption. The process by which gas molecules are drawn to and stick to the surface of a solid substance is known as adsorption. Due to the huge surface area of graphene, there are many adsorption sites for CO_2 molecules. For CO_2 adsorption, several graphene derivatives have also been investigated, including graphene oxide (GO) and reduced graphene oxide (rGO).

CO_2 adsorption by graphene and its derivatives is predominantly physisorption, which is a van der Waals interaction, a weak connection between molecules of similar sizes without a net charge that does not require the creation of chemical bonds, the sharing of electrons, or changes to the chemical structure of interacting molecules. Weak van der Waals interactions between the CO_2 molecules and the graphene surface power the physisorption process (Fig. 4). The pore size, surface area, and surface functions impact this interaction. GO has oxygen-containing functional groups on its surface, which can improve its physisorption of CO_2. By the reduction process, GO can reduce to rGO adding more defects and increasing available sites for physisorption (Lee and Park 2012; Ali et al. 2019; Ramar and Balraj 2022).

It has also been observed that temperature, pressure, and the presence of other gases are a few variables that affect graphene's ability to capture CO_2. Because the van der Waals interactions between the CO_2 molecules and the graphene surface diminish at higher temperatures, the adsorption capacity of graphene is reduced with temperature increase which also indicates an exothermic nature of physisorption. For physisorption, the binding energy lies between 20 and 40 kJ mol^{-1}. At lower pressures, the ability of graphene to adsorb declines due to reduced quantities of CO_2 molecules available for adsorption. Gases like N_2, O_2, CO, and CH_4, with similar kinetic properties, can compete with CO_2 molecules for adsorption sites, which can have an impact on the ability of graphene to selectively favor CO_2. However, the adsorption capacity of graphene is reduced due to the presence of moisture in the gas stream as they can block the adsorption sites and inhibit CO_2 facilitation on the adsorbent surface.

CO_2 adsorption by graphene can also occur by chemisorption. Chemisorption is a stronger interaction between molecules than physisorption which involves sharing of electrons and the establishment of chemical bonds between two compounds. This kind of adsorption is reliant on the electronic configuration and both the chemical structure and composition of the adsorbent and adsorbate materials. Through the creation of chemical connections between the carbon atoms in the graphene lattice and the oxygen atoms in the CO_2 molecule, graphene has demonstrated the chemisorption of CO_2 by reconfiguring its lattice structure to accommodate the formation of carbonyl and carboxyl groups from the captured CO_2 (Fig. 4). The binding energy for chemisorption is much greater than physisorption (80–40 kJ mol^{-1}).

CO_2 capture performance of graphene and its derivatives is also influenced by the introduction of functional groups, such as carboxyl, hydroxyl, and amine groups, on the adsorbent surface. Due to increased surface area and greater charge concentration exposed to the incoming CO_2 molecule, functionalized graphene has a higher CO_2 adsorption capacity than pristine graphene (Fraga et al. 2019) (Fig. 5). The introduction of hydroxyl and carboxyl groups

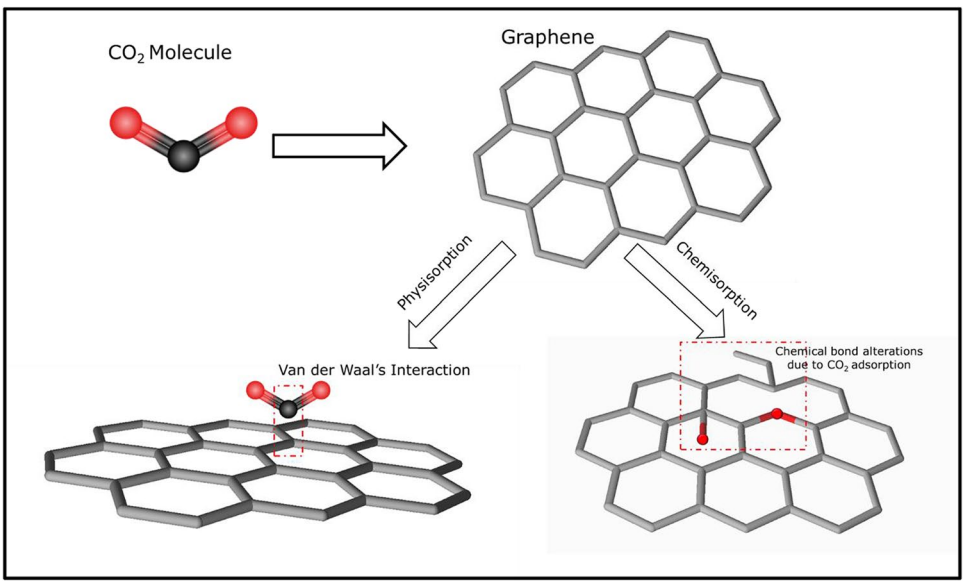

Fig. 4 CO_2 adsorption mechanisms (physisorption and chemisorption) by graphene

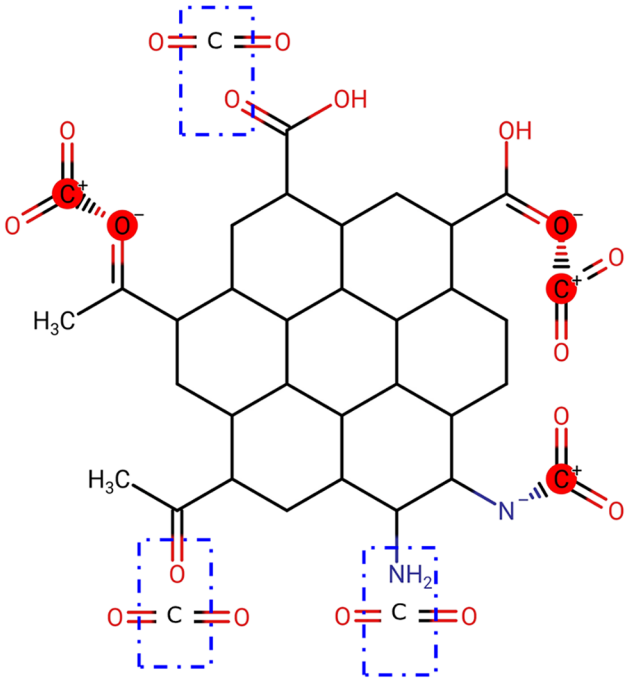

Fig. 5 CO_2 adsorption mechanism by various functionalization of graphene

on the surface of graphene improves its adsorption capacity of amoxicillin by up to 400% (Aguilar et al. 2021). Similarly, Fatihah et al. (2019) found that the introduction of amine groups on the surface of GO increased its CO_2 adsorption capacity by up to 80%.

Adsorption of CO_2 on graphene and its derivatives is predominantly physisorption. Dry conditions, low temperature, and high pressure are beneficial for the adsorption of CO_2 molecules. By adding defects or functional groups to the surface of graphene, one can boost the material's capacity for adsorption while also increasing the affinity of CO_2 molecules for the graphene surface.

DFT is a quantum mechanics–based computational method that can be used to calculate the electronic structure of molecules and materials. DFT is based on the density of electrons rather than wave functions, which makes it computationally efficient for larger systems as compared to GCMC. DFT can be used to calculate various properties such as electronic structure, geometry, and thermodynamics of materials. In the context of CO_2 capture, DFT in conjunction with molecular dynamic simulations can be used to investigate the adsorption mechanism, energy barriers, and the role of surface chemistry on CO_2 capture (Chakraborti and Pal 2014; Mino et al. 2014; Balasubramanian and Chowdhury 2015; Liu et al. 2015; Sun et al. 2015; Coello-Fiallos et al. 2017; Gupta et al. 2017; Li et al. 2017; Kamel et al. 2020; Wang et al. 2020; Baachaoui et al. 2021).

The pioneering study employing DFT simulation was carried out to analyze the adsorption of CO_2 on a single defective graphene sheet with a single vacancy defect by Pepa Cabrera. Demonstrating strong physisorption, the final configuration of a CO_2 molecule with a vacancy defect results in an estimated molecule binding energy of around − 136 meV. This value is lower compared to the binding energy of − 151 meV obtained for the same simulation on pristine graphene sheets, which indicates that the presence of defects improves CO_2 adsorption (Cabrera-Sanfelix 2009). This work has been built upon, by others since 2009, with variations including incorporation of dopants and functional groups on the adsorbent itself, gas mixtures instead of single species CO_2 as the sole adsorbate, and external field variations.

Investigating the selectivity trend of gas separation through nanoporous graphene (Liu et al. 2015), the authors used molecular dynamics simulations to study the separation of gases such as CO_2, N_2, and CH_4 through nanoporous graphene membranes with varying surface characteristics. The results showed that the pore size and shape are the primary factors influencing gas separation and selectivity. In particular, the selectivity of CO_2/N_2 separation increased as the pore size decreased, whereas the selectivity of CO_2/CH_4 separation increased as the pore size increased. It was also illustrated that the pore shape also affects the selectivity, with zigzag-shaped pores showing higher selectivity than armchair-shaped pores. Building upon this work, a nitrogen and hydrogen atom–doped graphene adsorbent with 12 graphene rings has been investigated for its gas separation capability of species involved in natural gas processing; the selectivity of the gases CO_2, H_2S, and N_2 is observed to be of the order 10^2 higher as compared to others.

The presence of dopants and functionalities has also been investigated by DFT and molecular dynamics simulation. Testing the effect of simultaneous doping of N, CO_2 capture performance of graphene (Li et al. 2017) utilized a combination of experimental and computational techniques to study the effect of both dopants on the structural, electronic, and adsorption properties of graphene. The results showed that the CO_2 adsorption capacity of graphene is improved due to doping of N and S, by creating additional adsorption sites and modifying the electronic structure of graphene. The authors also found that the optimal N/S doping ratio for maximizing the CO_2 adsorption capacity was 2:1. Functionalized armchair graphene nano ribbons were tested as CO_2 adsorbents using DFT while designing gas sensors (Salih and Ayesh 2020), which shows improvements in adsorption by almost 35 kJ mol^{-1} by incorporating O and OH functionalities on the surface of the adsorbent. Cooperative effects of metal-doped surface functional groups and the pore size effects have been investigated by use of both DFT and

GCMC studies (Chen et al. 2021), which shows phosphorus doping is better for CO_2 uptake.

DFT calculations have also been used to analyze the structural and electronic properties of graphene to attain further insights into its behavior; in one such study, graphene has been analyzed and compared to germanene in both single- and double-layer systems (Coello-Fiallos et al. 2017). The authors found that germanene exhibited stronger interlayer interaction than graphene in the bilayer system, resulting in a smaller interlayer distance and larger binding energy. The electronic properties of the two materials were found to be different, with germanene exhibiting a larger bandgap than graphene due to the buckling of its honeycomb lattice, which however reduces its capacity as a viable CO_2 adsorbent.

The effect of an external force field has also been investigated; in one such study analyses, phosphorus-doped graphene has been tested as CO_2 adsorbent in a controlled external electric field (Esrafili 2019), which indicates the change of adsorption energies from chemisorption to physisorption on removing the electric field. The difference in energies of 60 kJ mol^{-1} can also be applied to the same configuration for the CCS system. A similar study tested the potential of penta-graphene as a controllable carbon separation, capture, and storage material using a controlled electric field and utilized molecular dynamics simulations for studying CO_2 adsorption on penta-graphene under different electric field strengths (Wang et al. 2020). The results showed that the adsorption of CO_2 on penta-graphene was enhanced under an electric field (− 128.1 kJ mol^{-1}), and the selectivity for CO_2 over C_2N (− 21.05 kJ mol^{-1}) increased with increasing electric field strength. To test for CO_2 under realistic conditions inside an electrode for electrochemical reduction of Fe–N-graphene was analyzed as a CO_2 adsorbent using ab initio molecular dynamics simulation (Li et al. 2020a, 2020b), which provides adsorption energy of − 45.2704 kJ mol^{-1} in K-sol, indicating a strong affinity for CO_2 for the intended catalyst.

Some advanced studies have also been made possible due to the rapid growth and accessibility of computational resources, enabling the testing of materials beyond graphene; one such material is germanene, which has already been discussed in the previous section. Another such advanced material is graphyne, which has been speculated as a CO_2 adsorbent. Oxides of the same have been investigated as CO_2 adsorbent using DFT and MD simulations which indicated physisorption behavior (− 22.73 kJ mol^{-1}). Advanced studies have also been carried out to check changes in the adsorption behavior of CO_2 over graphene influenced by CO_2 clustering on adsorbent surfaces (Meconi and Zangi 2020; Zhang et al. 2022).

Functionalization of graphene with long-chain amines is a viable route to improve CO_2 adsorption capabilities; one such analysis highlights the interaction between graphene and amino acids (Kamel et al. 2020) using DFT calculations and MD simulations, and the researchers found that graphene and functionalized graphene nanosheets can interact strongly with certain amino acids through hydrogen bonding and pi-stacking interactions. This study indicates that the nature and strength of interaction are dependent on functional groups present on the graphene surface with the possibility of potential applications of graphene-based materials in the field of biotechnology. In conclusion, density functional theory (DFT) is a reliable tool that has made possible calculations investigating the mechanism of air capture by graphene and its derivatives (Table 1). By modeling the interaction of graphene-based materials with various air molecules, one can identify key factors that influence the adsorption properties, such as the nature of the graphene surface and functionalities attached to it. DFT calculations have also been used to predict the thermodynamic and kinetic properties governing the air capture process and are an invaluable tool for the design and optimization of graphene-based air capture materials. Overall, the use of DFT calculations enables prospective investigators to attain insights into the fundamental processes underlying air capture by graphene and its derivatives, which has important implications for the development of sustainable and efficient air capture technologies.

Adsorption performance of graphene-based materials derived from industrial grade precursors

Owing to its distinctive blend of physical and chemical properties of graphene, it has been established as an innovative material for the adsorption of CO_2. Its high mechanical and chemical stability makes it durable and able to withstand harsh conditions. Furthermore, graphene is a highly selective adsorbent, making it possible to target specific molecules such as CO_2. This has the potential to lead to more efficient and targeted removal of CO_2 from industrial processes or the atmosphere. Much research has already been done on obtaining varieties of graphene and related products to use as adsorbents. Graphene developed for air adsorption applications rely on industrial grade graphite as the carbon precursor, and this route is termed the top-down approach for synthesizing graphene and is summarized in Table 2. Mishra and Ramaprabhu (2012) utilized polyaniline-functionalized hydrogen exfoliated graphene (PANI-f-HEG) derived from pure graphite, demonstrating a high CO_2 adsorption capacity. The PANI-f-HEG sample was found to show adsorption of about 21.6 mmol/g CO_2 (at 25 °C and 11 bar pressure). However, using expensive graphite as a starting material stands out as one of the notable drawbacks.

Table 1 The use of DFT in investigating CO_2 adsorption by graphene and its derivatives

Aims of the work	Main methods used	Software packages employed	Key findings	References
Defective graphene sheets tested for adsorption of CO_2	DFT	VASP	Interaction of CO_2 with a vacancy defect on a monolayer graphene sheet provides a binding energy of − 136 meV (− 13.1 kJ mol^{-1}) in the optimized state, indicating physisorption	Cabrera-Sanfelix (2009)
Nanoporous graphene tested for its selectivity for gas molecules with sizes comparable to CO_2 based on their permeation fluxes	MD	LAMMPS (large-scale atomic/molecular massively parallel simulator)	The selectivity of the adsorbent for gas molecules was observed to be in the order of decreasing kinetic diameter of each species	Liu et al. (2015)
N and H doped graphene rings analyzed as gas sieving membranes, for natural gas processing; using multiple gas combinations of similar kinetic properties	MD	LAMMPS (large-scale atomic/molecular massively parallel simulator); the pair interactions modeled by the AIREBO potential	For all pore sizes considered, CO_2 and H_2S demonstrate higher permeance than N_2. Fluxes of permeating gases are observed to be much higher than non-permeating ones	Sun et al. (2015)
Graphene sheets with vacancy defects and N, S-dual doping tested as CO_2 adsorbents	DFT	VASP	The adsorption observed is higher than graphene with vacancy defect without dopant, indicated by adsorption energy of up to − 0.39 eV (− 36.56 kJ mol^{-1})	Li et al. (2017)
Functionalized arm chair graphene nanoribbons tested for CO_2 adsorption	DFT	ATK-VNL package	Pre surface modification adsorption energy of CO_2 on AGNR is − 0.145 eV (− 13.97kJmol^{-1}). Modification of the AGNR with O and OH changes this to − 0.538 eV (− 51.82 kJ mol^{-1})	Salih and Ayesh (2020)
Metal-doped functionalized graphite surfaces were investigated for the capture of CO_2 molecules	GCMC + DFT	$Dmol^3$ for DFT, SORPTION for GCMC	In the pressure range of 0–300 kPa highest overall CO_2 uptake is demonstrated by phosphorus doped surfaces Micropores capture CO_2 in low-pressure ranges, while mesopores become relevant at high pressures	Chen et al. (2021)
Phosphorus-doped graphene tested as CO_2 adsorbents. The effect of the electric field on the same was also investigated	DFT	$Dmol^3$ module embedded in Materials Studio software	An applied external electric field makes the adsorption energy reach − 0.78 eV(− 75.1 3 kJ mol^{-1}), which is indicative of a chemisorbed configuration. The removal of the electric field reduces this to − 0.10 eV (− 9.63 kJ mol^{-1}) which is indicative of a physisorbed configuration	Esrafili (2019)
CO_2 adsorption and separation capacity analysis carried out for penta-graphene nanosheet adsorbent in the presence of an external electric field	DFT	$Dmol^3$ module embedded in Materials Studio software	Electric field strength influences physisorption with the highest adsorption energy of − 1.330 eV (− 128.1 kJ mol^{-1}) observed for 0.04 au field strength. CO_2 coverage on penta-graphene nanosheet reduces the binding strength of incoming CO_2 molecules	Wang et al. (2020)

Table 1 (continued)

Aims of the work	Main methods used	Software packages employed	Key findings	References
Fe–N-graphene tested for CO_2 adsorption in electrochemical conditions inside an electrolyte	DFT	VASP	In a reactive K-sol, the adsorption energy is obtained as − 0.47 eV (− 45.2704 kJ mol^{-1}) which indicates chemisorption-like behavior	Li et al. (2020a, b)
Investigation of the electronic and structural properties of single- and double-layer graphene and a systematic comparison of free-standing germanene	DFT	Quantum Espresso with Nano-Lab add-on package	-	Coello-Fiallos et al. (2017)
Testing oxides of graphyne for CO_2 adsorption	DFT + MD	$Dmol^3$ module embedded in Materials Studio software	The best adsorption uptake of CO_2 was observed for graphyne oxide indicated by an adsorption energy of − 0.236 eV (− 22.73kJmol^{-1}), and the value indicated physisorption	Mofidi and Reisi-Vanani (2020)
Graphene surface tested for effect on CO_2 uptake due to adsorption induced clustering of CO_2	DFT + MD	GROMACS version 4.6.5	Above a critical surface coverage of graphene, the CO_2–CO_2 interactions augment the adsorption energy imparting high selectivity during the separation of gas mixtures; however, the overall adsorption reduces from − 21.5 to − 12.4 kJ mol^{-1} which is the energy of trimerization	Meconi and Zangi (2020)
Reaction mechanism and interaction of two CO_2 molecules analyzed on surface graphene defects	DFT	Quantum Espresso (QE) Package	The adsorption energy changes from − 0.37610 eV (− 36.22 kJ mol^{-1}) for 1st molecule of CO_2 to − 0.07584 eV (− 7.3 kJ mol^{-1}) for 2nd CO_2 molecule indicating a reduction in capacity due to the filling up of defects and repulsion between similar molecules	Zhang et al. (2022)

Table 2 CO_2 adsorption performance of graphene fabricated from top-down route

Precursor	Final product	Microporous area (m^2/g)	Surface area (m^2/g)	Avg particle size (nm)	T (°C)	P (bar)	CO_2 adsorption capacity (mmol/g)	Source
Pure graphite	PANI-f-HEG	-	-	-	25	11	21.6	Mishra and Ramaprabhu (2012)
					50		18	
					100		12	
Graphite powder	Graphene sheets	484	-	-	0	1	2.894	Chowdhury and Balasubramanian (2016)
	Graphene-based monolithic structures				25	1.013	2.1	Politakos et al. (2020)
Analytical grade graphite	HPGCs	209		3.8	0	1	1.76	Xia et al. (2014)
Industrial grade graphene oxide	GO functionalized with iodobenzene	825			20	1.013	1.24	Kumar et al. (2014)
Graphene oxide	LDO	-	-	9.25	200	-	0.35	Wu et al. (2022)
	LDO-SA			4.11			0.52	
	2GO-LDO-SA			3.89–4.08			0.59	
	4GO-LDO-SA						0.68	
	8GO-LDO-SA						0.74	
	6GO-LDO-SA						0.83	
Graphene	N-MGN	503–609	2521.72		25	0.4	10.59	Lyu et al. (2022)
						70	40.16	
	N-GOs:				50	1.013		Alghamdi et al. (2018)
	PPy/HCl-1: (polymer/KOH = 1:2)		1491	50–200			1.36	
	PPy/HCl-1: (polymer/KOH = 1:4)		2870				1.13	
	PPy/H_2SO_4: (polymer/KOH = 1:2)		1374				1.13	
	N-rGO-ZnO		1122		25	1.013	3.55	Li et al. (2016)
	S-doped microporous carbon material		1567				4.5	Chandra et al. (2012); Seema et al. (2014)
MR/GO composites	GO(0.25)/MR-500		1264		25	5	5.21	Ouyang et al. (2021)
	GO(0.25)/MR-600		972				04.29	
Graphene Oxide	Aminated graphene oxide (EDA)		2.73		30	1	1.1	Zhao et al. (2012)
	Cu-IFGO		123		25	2.1	2.1	Bhanja et al. (2016)
	Ultrasonic TEPA activated GO		194.84		65	0.1	1.2	Liu et al. (2019)
DAC-GO	DAC-0.05GO-PEI				25		0.78	Qiu et al. (2022)
	DAC-0.05GO-cPEI						4.25	

Table 2 (continued)

Precursor	Final product	Microporous area (m^2/g)	Surface area (m^2/g)	Avg particle size (nm)	T (°C)	P (bar)	CO_2 adsorption capacity (mmol/g)	Source
Graphene Oxide	Graphene			80			0.5–1	Stankovic et al. (2022)
	Composite of rGO and polymers (NaSS and AMPS)	183–207				1.013	1.01	Politakos et al. (2020)
	Hybridization of MOFs with GO:				0	0.15		Zhao et al. (2022)
	C-10						5.88	
	Pure CuBTC (C-0)						1.6	
	MOF/GO-U3		1367		20	15	13.41	Policicchio et al. (2014)
					0	1	8.45	Zhao et al. (2014)
					22		4.75	
	MOF/GO-U2		936		0		5.38	
					22		2.97	
	MOF/GO-U1		864		0		4.02	
					22		2.3	
	MOF/GO		1010		0		5.52	
					22		3.09	
	LDH nanoparticles precipitated onto GO	55.8		30	300		1.23	Garcia-Gallastegui et al. (2012)

In a study conducted by Chowdhury and Balasubramanian (2016) they investigated the use of graphene sheets derived from graphene powder through an enhanced version of the Hummer's method and synthesis by hydrazine reduction of graphene oxide. The extremely hydrophobic graphene sheets interconnected by hierarchical pore networks exhibited an adsorption capacity of 2.894 mmol/g at 25 °C and 1 bar pressure. Politakos et al. (2020) put forward using graphene-based monolithic nanostructures obtained from GO nanoplatelets as adsorbent material. Under similar conditions of temperature and pressure, the material showed an adsorption capacity of 2.1 mmol/g. Hierarchical porous graphene-based carbons (HPGCs) obtained from analytical grade graphite have been used by Xia et al. (2014) as an adsorbing material. In this case, too, the GO is obtained using the modified Hummer's method. At 0 °C and 1 bar pressure, the material has been found to adsorb 1.76 mmol/g of CO_2. However, the reusability of this material remains a matter of question.

Reduced graphene oxide (RGO) has also been used as an adsorbent for CO_2 in several instances. With industrial-grade GO as a precursor, Kumar et al. (2014) prepared rGO by $NaBH_4$ reduction of graphene oxide. They subsequently employed the Sonogashira coupling strategy for synthesizing durable, porous, and robust graphene frameworks with organic linkers. Iodobezene functionalization of GO sheets was done using diazonium salt of 4-iodoaniline. This process resulted in the incorporation of iodobenzene functional groups on both sides of rGO, forming rGO-IBz. At 20 °C, 1 atm pressure, the material had a CO_2 adsorption capacity of 1.24 mmol/g. The adsorption performance of nanocomposites of GO-doped stearate-intercalated layered double oxides (LDO) was studied by Wu et al. (2022), and their adsorption capacity at 200 °C indicated that a GO/LDO ratio of 6:1 had the best adsorption capacity. To activate the adsorbents before CO_2 adsorption, they underwent a calcination process using a tube furnace. The calcination was carried out

in a nitrogen flow of 50 ml/min at a temperature of 400 °C for a duration of 4 h.

Doping of GO with nitrogen is also one of the emerging adsorbents for CO_2 capture. The process of synthesizing polypyrrole functionalized graphene sheets involved chemically polymerizing pyrrole in graphene oxide. This synthesis was achieved through the utilization of ammonium persulfate as an initiator, followed by subsequent reductions using hydrazine. Its CO_2 adsorption capacity was observed to be 4.3 mmol/g at 25 °C, 1 bar pressure (Chandra et al. 2012). A variety of nitrogen-doped graphene oxide sheets (N-GOs) were tested by Alghamdi et al. (2018) which yielded interesting results. Monomers were mixed with a fixed quantity of desired dopant (HCl, H_2SO_4, C_6H_5-SO_3-K), the mixture was stirred and added with ammonium persulfate dissolved in water. The prepared polymer was carbonized. Among the varied sample materials developed, a polymer to KOH ratio of 1:2 yielded a CO_2 adsorption of 1.36 mmol/g at 50 °C and 1 atm pressure, while it decreased to 1.13 mmol/g for a polymer to KOH ratio of 1:4. Upon comparing the obtained adsorption values with those reported in previous studies, it was found that the adsorption capacities of N–GOs were marginally lower. This finding is a clear indication of the potential for improvement of these materials' adsorption properties.

Zinc oxide-based N-doped reduced graphene oxide (N-rGO-ZnO) (Li et al. 2016) has been found to adsorb 3.55 mmol/g CO_2 at 25 °C and 1 atm pressure. To synthesize N-rGO, a combination of GO and melamine was utilized. The inclusion of melamine served to create a charged layer that attracted the negatively charged GO via electrostatic interaction. Carbon materials doped with nitrogen or sulfur, developed by the Kwang Group, exhibited enhanced selectivity in capturing CO_2 (Seema et al. 2014). S-doped microporous carbon materials formed by chemical activation of an rGO/PTh (thiophene) material (SG) on undergoing adsorption tests yielded a CO_2 adsorption capacity of 4.5 mmol/g (Seema et al. 2014) under similar conditions. For synthesizing rGO, hydrazine reduction was employed. The necessary quantities of reduced graphene oxide and thiophene were dispersed in chloroform at room temperature using sonication. The synthesis of PTh was conducted using a comparable procedure, excluding the presence of reduced graphene oxide. Subsequently, the activation of SG was accomplished by utilizing a predetermined concentration of potassium hydroxide solution (Zhu et al., 2011; Raymundo-Piñero et al. 2005). Following 9 cycles, the material exhibited an initial decline of 10% in its adsorption capacity, which was subsequently recovered. This decline in adsorption capacity can be attributed to the instability of different oxidation states that sulfur can undergo during rigorous activation procedures. In a related study conducted by Ouyang et al. (2021), they focused on a material with some similarities. They utilized a unique nitrogen-doped porous carbon material derived from composites of melamine-resorcinol–formaldehyde resin and graphene oxide (MR/GO) as a precursor. To obtain a nanoporous carbon membrane (NPCM) derived from GO/MR, with a substantial surface area and abundant pores, the activation process was performed under an N_2 stream using KOH as the activating agent. Final-stage carbon materials were obtained with activation temperatures of 500 °C. The developed sample adsorbed CO_2 to an extent of 5.21 mmol/g at 25 °C and 500 kPa, while under similar conditions, NPCM activated at 600 °C showed CO_2 adsorption of about 4.29 mmol/g. The exceptionally rapid kinetics observed in these materials indicate that the previously synthesized material offers the advantage of reducing the adsorption cycle time, which holds promising implications for practical applications.

Recently, a variety of experiments have been conducted to test the adsorption capacity of GO functionalized with different kinds of amines such as ethylenediamine (EDA), diethylenetriamine (DETA), and triethylenetetramine (TETA). Zhao et al. (2012) found the best performance with EDA. Synthesizing graphene with a modified Hummer's method, the GO products were divided based on concentration in the aqueous solution. A pre-determined amount of EDA, DETA, or TETA was added to each solution, and finally, the modified GO was isolated by centrifugation. EDA functionalized GO adsorbed CO_2 up to 1.1 mmol/g at 303 K temperature and 1 bar pressure. Tuning of operating conditions may lead to improved performance. Bhanja et al. (2016) explored an additional innovative material that revolves around amine functionalized graphene oxide. Their study focused on copper-grafted imine-functionalized graphene oxide (Cu-IFGO), which was obtained through post-synthetic modifications involving the co-condensation of 3-aminopropyltriethoxysilane (APTES). This material exhibited an adsorption capacity of 2.1 mmol/g at 298 K and 1 bar pressure. GO functionalized by a combination of a two-step process consisting of physical activation by ultrasound and chemical activation with TEPA to yield ultrasonic-TEPA activated GO, which has been found to have a CO_2 adsorption capacity of 1.2 mmol/g (Liu et al. 2019) at 338 K temperature and 0.1 atm. One should bear in mind the criticality of regenerating an adsorbent both from an economic perspective and for prolonged utilization. In this specific instance, the cyclic adsorption/desorption data revealed the notable stability of TEPA-GO's adsorption behavior, with a mere 1% reduction in adsorption capacity observed after 10 cycles. However, practical applications ask for a higher number of cyclical tests, which may lead to a reduction in adsorption capacity. DAC-GO-PEI formed by the impregnation and crosslink of polyethyleneimine (PEI) into a dialdehyde-cellulose/graphene oxide composite gel also acts as a good adsorbent (Qiu et al. 2022). On oxidation using $NaIO_4$, thin cellulose

nanofiber was found to gather into a strong dialdehyde cellulose network. To assess the impact of GO, the aldehyde group content of gels was measured using a titration method. At 25 °C, 4.25 mmol/g of CO_2 was found to be captured by DAC-0.05GO-cPEI. But the dependency of the performance of the resultant product on GO being utilized is a problem.

Stankovic et al. (2022) used an industrially sourced aqueous dispersion of GO of 4 mg/mL to yield GO/polymer composites as adsorbents, where nanocomposites were functionalized with technical monomers; methyl methacrylate (MMA) and butyl acrylate (BA), sodium 4-vinyl benzenesulfonate (NaSS), glycidyl methacrylate (GMA), 2-hydroxyethyl methacrylate (HEMA), and 2-aminoethyl methacrylate hydrochloride (AEMH) were used as functional monomers. In the synthesis process, tert-butyl hydroperoxide solution (TBHP) and L-ascorbic acid (AsA) were employed as redox initiators, while sodium dodecyl sulfate (SDS) and hexadecyl trimethyl ammonium chloride (HAC) were used as demulsifiers. Sodium bicarbonate ($NaHCO_3$) was used as a buffer. At 25 °C, the material exhibited an adsorption performance of 0.5–1 mmol/g. Politakos et al. (2020) used three-dimensional monolithic composite structures composed of reduced graphene oxide and polymer (NaSS and AMPS), copolymerized with the monomer MMA. This material also showed a similar CO_2 adsorption of 1.01 mmol/g under similar temperatures and conditions.

Cu-BTC and its composites with graphite oxide forming MOF/GO-Urea stand out as good adsorbents. Testing was carried out on a variety of composites with increasing amounts of urea used for the synthesis of Cu-BTC as mentioned in the literature (Chui et al. 1999). Experiments conducted at 273 K and 295 K at 0.1 MPa, showed adsorption of 8.45 mmol/g CO_2, which was the highest among all combinations of MOF/GO and urea. Just by a slight tweak in the conditions, Policicchio et al. (2014) put forward that the same composite can adsorb about 13.41 mmol/g CO_2 at room temperature and 1.5 MPa pressure; this increase in the required operating pressure is a drawback for direct air capture applications. Garcia-Gallastegui et al. (2012) used layered double hydroxide (LDH) nanoparticles precipitated onto graphene oxide as CO_2 adsorbent. By dispersing a fixed quantity of GO in an aqueous solution containing pre-determined concentrations of NaOH and Na_2CO_3, a colloidal dispersion of negatively charged GO nanosheets was achieved. This dispersion served as the basis for preparing four different LDH/GO hybrids, with varying weight percentages of GO. Upon conducting tests at a high temperature of 573 K, an adsorption capacity of 1.23 mmol/g was obtained. It is important to note that for applications involving synthesized LDHs in temperature swing processes like precombustion carbon capture and storage (CSS) and sorption-enhanced hydrogen production, the optimization of adsorption and regeneration temperatures is essential. While a low adsorption temperature and a high regeneration temperature can result in maximum adsorption capacity, it can lead to energy inefficiency and create thermal gradients Thus, lack of energy efficiency remains a notable limitation in this case.

Graphene and graphene derivatives sourced through the top-down route have demonstrated exceptional CO_2 adsorption capability (up to 40 mmol/g). However, nearly all of the synthesized materials require very high-quality industrial grade precursors which inhibit the production of these adsorbents at a bulk scale due to economic constraints. Hummer's method involved in the synthesis of GO from graphite and subsequent hydrazine reduction also relies on expensive chemicals which further drive up the process costs. For this material to be widely accepted and implemented at an industrial scale to combat pollution, the costs involved in the fabrication process need to be reduced.

Graphene from natural, organic, and plastic waste sources

Graphene, GO, and graphene derivatives of carbon obtained from the top-down route rely on industrially sourced precursors, with a dependence on harsh and non-environment friendly chemicals involved throughout the route of synthesis. This not only increases the cost but creates a negative environmental impact. An alternate procedure named the bottoms-up route is a viable alternative. This route involves sourcing the carbon from organic and natural materials (mostly organic wastes) and also from plastic wastes. This method allows for the valorization of wastes generated from daily life and also contributes to the removal of plastic wastes from the environment (Table 3).

Macro-algae derived graphene adsorbent was obtained using KOH activation at a carbonization temperature of 400 °C, carbon and hydroxide ratio of 1:4, and activation of the blend at a temperature of 850 °C, which yielded porous graphene of about 1411 m^2/g specific surface area and CO_2 uptake capacity of 2.78 mmol/g at 30 °C and 1 bar pressure (Fig. 6). Characterization techniques undertaken for the samples (SEM, TEM, AFM, BET, XRD, Raman spectroscopy, XPS) show carbon-based graphene-like sheets, very similar to multi-layered graphene sheets. On carrying out CO_2 adsorption tests, the exhibited CO_2 uptake capacity is per the graphene sheet-like structure obtained. Though adsorption was not investigated by functionalizing the same, variations to pore structure and surface chemistry were investigated with changes in activation temperatures. This study has opened up the possibility of utilization of local macroalgae populations as an abundant and sustainable carbon precursor feedstock (Ai et al. 2021). Using the starting material wheat, few-layered graphene was fabricated by

Table 3 Graphene and graphene derivatives from the bottoms-up route

Precursor	Method	Final product	Defining characteristics	Key advantages	Possible pathways for CO_2 capture	Reference
Macro-algae	Carbonization, KOH treatment	Pristine graphene sheets	• **Microporous area** of 1075m^2g^{-1} (**BET** surface area of 1411m^2g^{-1}) • **Average pore size** of 3.30 nm • **CO_2 adsorption capacity** of 2.78 mmol/g	• Does not require the use of Harsh chemicals • Production is quick	The sheets may be further functionalized and the improvements to the air capture capacity may be investigated	Ai et al. (2021)
Wheat straw	Hydrothermal treatment, pyrolysis (under N_2 atmosphere), graphitization	FLG	• Graphene **sheet thickness**: 1.2 nm • **BET surface area**: 35.5 $m^2\ g^{-1}$ • **Total pore volume**: 0.10 $cm^3\ g^{-1}$ • **Yield**: ca. 11.3 wt%	• Complete graphitization ensured by the use of a Graphite Reactor in the final stage which reaches 2600 °C • Porosity in FLG provides a large amount of In-situ active sites obtained due to the high porosity of FLG	The produced FLG may be tested for CO_2 capture capability	Chen et al. (2016)
Disposable paper cups	KOH treatment, ion exchange with Fe2 + [$(NH_4)_2Fe(SO_4)_2$ as a Fe source], **HCL**	Graphene Sheets (FLG)	• Graphene **sheet thickness**: 1 µm (AFM) • **Conductivity value**: 470 Sm^{-1} (Four probe Method)	• Metal Nanoparticles dopants are distributed uniformly on the FLG • Graphene sheets obtained from waste have low defects and high crystallinity	An alternate chemical in place of **$(NH_4)_2Fe(SO_4)_2$,** may be used to facilitate N-doped graphene which may be tested for air adsorption capacity	Zhao and Zhao (2013)
Dead camphor leaves (*Cinnamomum camphora*)	One-step pyrolysis	Few-layer graphene (FLG)	• **Sheet thickness**: 2.37 nm • **BET** surface area: 296 m^2/g • **Yield**: 0.8%	• The FLG sheets have a thickness of 7 layers • FLG is obtained as a suspension in Chloroform (stabilized by D-Tyrosine) • BET test confirms a nano-structure powder	The CO_2 adsorption capacity of the seven-layer thick FLG may be investigated	Shams et al. (2015)
Wood, leaf, bagasse, fruit, newspaper, bone, and **cow dung waste**	Carbonization, graphitization, Hummer's method, hydrazine reduction	GO and rGO **sheets**	• rGO sheets of a width of about 4-monolayer carbon thickness (confirmed via AFM) observed	• rGO sheets have consistent properties independent of the carbonaceous source • The temperature requirement during graphitization is restricted to within 500 °C	CO_2 adsorption experiments may be carried out on the rGO sheets to test for adsorption performance	Akhavan et al. (2014)

Table 3 (continued)

Precursor	Method	Final product	Defining characteristics	Key advantages	Possible pathways for CO_2 capture	Reference
Waste dry cell battery	**HCL** and **HNO_3** cleaning of waste zinc-carbon dry cell batteries, Hummer's method, hydrazine reduction	rGO	• rGO obtained in a black powder form • **Specific capacitance value:** 48 μ Fg^{-1} • **Electroconductivity:** 478.78 mS cm^{-1}	• No heating is involved in the process	rGO obtained may be polymerized to obtain aerogels and tested for CO_2 adsorption	Roy et al. (2016)
Coconut shell and coconut coir	Catalytic oxidation with **ferrocene**, thermal annealing	Well graphitized rGO sheets (2D material structure)	• **Specific capacitance value:** 11.1 F/g(CCF) and 60.2 F/g(CSF) • **Interlayer distance**: 3.8 Å (CCF) and samples it is 3.6 Å (CSF) • **Cycles:** 3000 • **Capacity retention:** 99%	• rGO sheets tested as supercapacitors with good performance	rGO may be tested as an effective CO_2 adsorbent	Tamilselvi et al. (2020)
Agricultural wastes (orange peel, sugarcane bagasse, and rice bran)	Catalytic oxidation with **ferrocene**	GO	• The **average grain sizes**: 23.99 nm (**orange peel**),15.5 (**sugarcane bagasse**), 2.235 nm (**rice bran**), and 1.77 nm (**tri-composite waste**) • **Interlayer distance**: 3.0442 Å (**orange peel**), 2.4737 Å (**sugarcane bagasse**), 2.0003 Å (**rice bran**) and 6.962 Å (**tri-composite waste**)	• GO was synthesized at a relatively low temperature (400 °C) • This method highlights the possibility of valorization of solid agro-waste without the need for sanitization	GO obtained may be further reduced to rGO or functionalized and utilized for air adsorption applications	Hashmi et al. (2020)
Rice husk biomass	Heat treatment, NaOH treatment	Graphene quantum dots (GQD)	• **Yield**: 15%	• The fabricated GQDs form stable dispersions in water, exhibiting bright and tunable photoluminescence • The Silica nanoparticles obtained as the byproduct can also be utilized	Using KOH instead of NaOH provides a route to obtain GO which may be tested as CO_2 adsorption materials	Wang et al. (2016)

Table 3 (continued)

Precursor	Method	Final product	Defining characteristics	Key advantages	Possible pathways for CO_2 capture	Reference
Bagasse	Mixing with **melamine**, hydrothermal treatment, **pyrolysis** (under **argon** atmosphere), chemisorption (sulfur)	N-doped graphene like carbon sheets	• Carbon structure like graphene sheets containing 4–8-layer graphene (observed from SEM) • Sulfur Loaded N-doped carbon sheets display: • **Reversible capacity:** 1169 $mAhg^{-1}$ with • **Capacity retention:** 77% • **Cycles:** 200	• The amount of melamine controls the exfoliation rate, surface area, and nitrogen content • Sulfur loading (battery performance) can be controlled by stacking multiple layers of N-doped carbon sheets	N-doped carbon sheets may be utilized for CO_2 adsorption applications	Babu and Ramesha (2019)
Microcrystalline cellulose	Development of cellulose aerogel (composited with a phenolic resin), carbonization	Novel graphene Aerogel	• **Yield**: 48% • **Specific area**: 1426.11 m^2/g • **Total pore volume**: 1.02 cm^3/g	• Graphene aerogel preparation makes use of Sol–Gel reaction • Stable network structure is developed in cellulose aerogel (due to phenolic resin)	A phenol substitute may be used to reduce environmental hazards, and the final product may be tested as a CO_2 adsorption material	Li et al. (2020a, b)
Waste chicken fat	Dry-rendering process, LPCVD, electrochemical delamination, acetone wash	Unified Mono Layer Graphene Film	• **Sheet resistance**: 300 Ω/square (the four-probe method)	• Deposited Graphene is continuous and without defects and contaminants • Raman spectroscopy shows a high degree of graphitization ($I_D/I_G < 0.1$) • The graphene obtained was crystalline and with high conductivity	The MLG may be doped, functionalized, and tested for CO_2 adsorption applications	Rosmi et al. (2016)
Raw carbon precursors used without pretreatment (cookies, chocolate, grass, plastics, roaches, and dog feces)	Spin coating (PMMA carbon source), CVD onto a Cu film	A single uniform layer of graphene	• **Sheet resistance**: 1.5–3.0 kΩ (the four-probe method)	• High-grade graphene with minimal defects and up to 97% transparency • Requirement of temperatures between 800 °C and 1000 °C • Yield is dependent on the size of the tube furnace	The MLG may be doped, functionalized, and tested for CO_2 adsorption applications	Ruan et al. (2011)

Table 3 (continued)

Precursor	Method	Final product	Defining characteristics	Key advantages	Possible pathways for CO_2 capture	Reference
Coal tar pitch	Spin coating, annealing (thermal CVD on Ni), etching of Ni using $FeCL_3$	MLG and FLG	• **Sheet resistance**: 1 kΩ/square (the four-probe method)	• Electrodes had 0.43 eV of hole injection barrier • Waste hydrocarbon source was used instead of explosive hydrocarbon precursors	The MLG may be doped, functionalized, and tested for CO_2 adsorption applications	Seo et al. (2015)
Polymers and plastic waste	CVD	High-quality freestanding graphene foil (GF)	• **Sheet thickness**: 1.7 to 2.8 µm • **Electroconductivity:** 3824 Scm^{-1} • **Carbon content**: 98–99%	• GF may be handled without a substrate due to microscale thickness • GFs prepared using varying plastic precursors have consistent structural properties • The foils exhibit flexibility and moldability	Produced Foils have the potential to act as excellent free standing CO_2adsorbents, and may be tested for the same	Cui et al. (2017)
Soybean oil precursor	CVD	Single-to-few layer graphene	• **Domain sizes**: 200–500 nm • **Sheet resistance**: 324 Ω/square (the four-probe method)	• Graphene obtained is a good Electrochemical genosensing electrode • Requires the use of a novel quartz tube • Continuous graphene films composed of SLG and FLG	Similar organic precursors may be utilized for the preparation of continuous graphene films and CO_2 adsorption may be investigated	Seo et al. (2017)
Graphite rods from empty mosquito repellent refills (Good Knight)	Electrochemical exfoliation, sodium citrate treatment	FLG	• Optimum voltage: 4.75 V (for electrochemical exfoliation) • **Interlayer distance**: 1.8 nm	• Graphene obtained has small quantities of oxygen based functional groups	Obtained graphene may be tested as CO_2 adsorbents	Udhaya Sankar et al. (2018)
Pencil cores	Electrochemical exfoliation	GO flakes	• Morphology: wrinkled or folded with 1–5 layers (TEM) • The **average grain sizes**: 1–5 µm (SEM)	• Good electrocatalytic activity and toxicity tolerance during the reduction of oxygen functionalities • Oxygen functional groups observed on the GO surface	Results are promising for mass production of GO which may be tested for CO_2 adsorption applications aided by the present surface functionalities	Liu et al. (2013)

Table 3 (continued)

Precursor	Method	Final product	Defining characteristics	Key advantages	Possible pathways for CO_2 capture	Reference
Mango peel	Plasma-enhanced CVD(PE-CVD)	High-quality Graphene		• High-quality graphene at lower temperatures (<400 °C) compared to conventional CVD methods • Longer exposure to plasma forms monolayer Graphene	Obtained Graphene may be tested as CO_2 adsorbents	Shah et al. (2018)
Waste car bumper and TiO_2 nanoparticles	Catalytic thermal decomposition	TiO_2 decorated rGO composites	• **Microporous area** of 120.3m^2g^{-1}(**BET**) • **Average pore size** of 18.56 nm	• Work focused on developing and testing TiO_2 embedded rGO and testing for Methylene Blue removal performance	Material developed has the possibility and should be tested as both CO_2 capture and conversion system	Mohamed and Alsanea (2020)
Empty PET water bottles (polyethylene terephthalate (PET) waste)	Pyrolysis, KOH activation, co-precipitation	Activated graphene (AG), nano- ferromagnetic activated graphene (NFMAG)	• **Microporous area**:319.62 to 460.01m^2g^{-1}(**BET**) • **Average pore size**: 1.981 nm to 2.177 nm with a total pore volume of 0.2315 cm^3g^{-1} • **Adsorption Capacity:** Methylene blue capture capacity of up to 348.3 mgg^{-1} for **AG** • **Operating Parameters:** 25 °C, pH of 10, and loading of 0.2 mg mL^{-1}	• Adsorption results indicated adherence to Langmuir Isotherm • NFMAG showed improved adsorption of Methylene Blue as compared to normal graphene (with better surface characteristics) due to the presence of Magnetite	Adsorption tests carried out were for MB dye. CO_2 adsorption may be tested	Mensah et al. (2022)

Table 3 (continued)

Precursor	Method	Final product	Defining characteristics	Key advantages	Possible pathways for CO_2 capture	Reference
Oil palm (*Elaeis guineensis*) biomass	Pulping, separation, and carbonization of lignin powder	Lignin derived graphene oxide	• **Microporous area:** 280.1 m^2g^{-1}**(BET)** • **Pore volume:** 0.222 cm^3g^{-1} • **Average pore size:** 3.15 nm • **Current density:** 15.65 mAm^{-2} • **Heavy metal removal:** 83.50% of Cd (II) (80 days)	• A readily available source of waste palm oil biomass is used as a carbon precursor • Microbial fuel cells (MFC) with palm oil sourced LGO anodes displayed a current density of more than 15 mAm^{-2} • Operation with 100 ppm Cd(II) solution also indicated heavy metal removal efficiency of more than 80%	The GO obtained may be tested as adsorbents for CO_2, and the surface characteristics may be further improved with the introduction of long-chain molecules (amines, organic acids, etc.)	Yaqoob et al. (2021)
Coal tar pitch	Dispersion into ethyl acetate, carbonization after addition of expanded vermiculite	Carbon nanosheets (CNS)	• **Specific surface area:** 297 m^2g^{-1}**(BET)** • **Pore volume:** 0.558 cm^3g^{-1} • **Reversible capacity:** 623 mAh g^{-1} ($2Ag^{-1}$) • **Capacity retention:** 99.7% • **Cycles:** 200	• Coal tar pitch-based carbon nanosheets show exceptional performance as anode materials for lithium-ion batteries, with 1147$mAhg^{-1}$ initial reversible capacity at 0.05 Ag^{-1} and 510$mAhg^{-1}$ rate capability at $2Ag^{-1}$	The CNSs may be used as CO_2 removal materials	Wang et al. (2021)
Cellulose filter paper	M500 CO_2 50 W laser engraver (line scan swing) on fire-protected filter paper	laser-induced graphene (LIG)	• **Sheet resistance**: 71.6 Ω/square (the four-probe method) • **Raman spectra: ~ 1 (I_D/I_G)**	• Laser induction has been used to produce high-quality graphene • Strain and bending functionality tested	The graphene developed may be modified and tested as CO_2 adsorbents	Kulyk et al. (2021)
Miscanthus grass	Pyrolysis, edge carboxylation (ball mill, CO_2 environment), ultrasonic exfoliation	GO (~ 10% monolayer) and GQD	• **Raman spectra: 0.94–0.95 (I_D/I_G)** • **Interlayer distance**: ~ 0.39 nm • **Sheet thickness:** 0.449–4.091 nm	• A single-step method is used to obtain multiple graphene derivatives • The product constituent proportions may be controlled by altering the synthesis condition	Derivatives with a sheet-like morphology are a viable candidate for CO_2 adsorption	Yan et al. (2021)

Table 3 (continued)

Precursor	Method	Final product	Defining characteristics	Key advantages	Possible pathways for CO_2 capture	Reference
Plastic waste mix	Shredding, cleaning, two-stage pyrolysis (mixture of bentonite nano-clay)	Graphene nanosheets (GN)	• **Corrugated-edged individual sheets of varying area** • **Raman spectra: 0.91 (I_D/I_G)** • **Interlayer distance**: ~ 0.39 nm • **Specific capacitance:** 398 Fg^{-1}(0.005 Vs^{-1})	• Fabricated GNs used as supercapacitors and dye-sensitized solar cells (DSSC)	The substrate is a viable candidate as a direct air CO_2 absorbent	Pandey et al. (2021)
***Hibiscus sabdariffa* sticks**	Carbonization, KOH activation, pyrolysis (argon atmosphere), HCL washing	Porous graphene like carbon sheets	• **Specific surface area:** ~ 2300 m^2 g^{-1}**(BET)** • **Pore volume:** 1.3 cm^3 g^{-1} • **Average pore size:** 2.2 nm • **Interlayer distance**: ~ 0.34 nm • **Specific capacitance value:** 240 Fg^{-1} (1 Ag^{-1}) • **Capacity retention:** 93% • **Cycles:** 25,000	• Fabricated sheets are tested as electrodes with high energy density (21.37 $Whkg^{-1}$) and high power density (13,420 Wkg^{-1})	High surface area (~ 2300m^2g^{-1}) sheets have the possibility of being utilized as CO_2 capture material	Nanaji et al. (2021)
Waxed cork	CO_2 infrared laser treatment (50 W, 1.06 µm, 2.0″ lens)	Porous three-dimensional laser induced graphene (LIG)	• **Raman spectra:** 0.5 (I_D/I_G) • **Specific capacitance value:** 1.35 mF cm^{-2} (5 m Vs^{-1}) • **Capacity retention:** 106% • **Cycles:** 10,000	• Wax-based ink pre-treatment on cork eliminates the need for mechanical supports required during electrode formation	The three-dimensional porous LIG may be used as a self-supported CO_2 capture device	Silvestre et al. (2022)
	Nd:YAG fiber laser treatment (50 W, 1.06 µm, 2.0″ lens)		• **Raman spectra:** 0.2 (I_D/I_G)			
Waste dry cell battery and pencil cores	Electrochemical exfoliation (lime juice and H_2SO_4 electrolyte), thermal treatment (650 °C)	Reduced graphene oxide modified with citric acid (CrGO)	• **Raman spectra:** 0.287 (I_D/I_G) • **Crystallite size:** ~ 17.0352 nm • **Surface roughness:** 0.49690 nm (AFM)	• Specific applications of the synthesized substrate are yet to be tested	Functionalized rGO has the potential to be a good CO_2 adsorbent and may be tested for the same	Singh et al. (2023)

Table 3 (continued)

Precursor	Method	Final product	Defining characteristics	Key advantages	Possible pathways for CO_2 capture	Reference
Date syrup	Heating (concentrating syrup), KCL treatment, controlled vacuum heating (N_2 atmosphere), washing	3D networked graphene foam	• **Specific surface area:** ~ 650 $m^2\ g^{-1}$**(BET)** • **Pore volume:** 0.395 $cm^3\ g^{-1}$ • **Raman spectra:** 0.74 (I_D/I_G) • **Average particle size:** 6 nm	• Applications are yet to be tested, only characterizations have been carried out	High surface area graphene network may be tested for CO_2 adsorption performance	Abed et al. (2023)

hydrothermally treating the precursor followed by carbonization and subsequent graphitization. Hydrothermal treatment was carried out inside a stainless-steel autoclave with Teflon lining at 150 °C for 6 h (Fig. 6). High-temperature pyrolysis was carried out at 800 °C for 3 h in a nitrogen atmosphere with KOH. The product was then dried inside a vacuum oven before thermally heating it inside a graphite furnace with Argon atmosphere blanketing at 2600 °C for 5. The yield was about 11.3 wt%, with a BET surface area of 35.5 m^2/g; the nitrogen adsorption–desorption isotherm showed hysteresis at 0.8 to 0.95 relative pressure indicating mesopores (attributed to KOH activation). Besides, a very thin layer of carbon (1.2 nm) indicated a bi- and tri-layer, sheet thickness, and elementary analysis along with XRD, and XPS indicates the formation of almost pristine FLG with high-degree graphitization (Chen et al. 2016). This method does not involve harsh chemicals, but a graphite reactor with a temperature requirement of 2600 °C is highly cost sensitive. Disposable paper cups provide another route to produce high-quality graphene sheets in bulk. Chemical treatment of paper pulps includes blending with KOH followed by $(NH_4)_2Fe(SO_4)_2$ which will coordinate the pulp with Fe^{2+} ions. The pulp is then graphitized (Fig. 6). Dense Fe_3C layers are formed due to the incorporation of a portion of carbon atoms into the iron phase. A rigid two-dimensional carbon atom layer (like graphite) manifests on the surface of iron layers due to the outward diffusion of carbon atoms upon lowering the temperature. The composite sheets are multi-layered, and treating the same with HCL removes the iron-producing high-quality graphene sheets. Compared to conventional routes, the yield of graphene sheets obtained per unit energy consumption is high. The sheets have low defects with high crystallinity and may be utilized as CO_2 adsorbents (Zhao and Zhao 2013). Another route to high-quality graphene sheets involves one-step pyrolysis of dead camphor leaves (*Cinnamomum camphora*). The sample is mixed with D-tyrosine and trichloromethane, to precipitate amorphous carbon (Fig. 6). A few-layered graphene (FLG) remains suspended in chloroform confirmed by TEM images, which may be filtered to obtain FLG; a strong acid or base may be used to wash away the tyrosine. The graphitization reaction occurs directly on the carbon precursor surface. The graphene obtained is attributed to the morphology of the dead leaves which reveal a porous structure when investigated (due to the cleavage of hemicellulose under nitrogen), and the thin layers are a possible source of surface for graphene growth. The BET gives the surface area of the FLG to be about 296 m^2/g, with a yield of 0.8%. The typical thickness obtained via AFM is about 2.37 nm corresponding to 7 layers of graphene. ID/IG ratio observed is 0.99 which is close to 0.845 of pristine graphene. The suspension obtained remains stable for 60 days (Shams et al. 2015). Plastic waste mix pyrolyzed with bentonite nano-clay

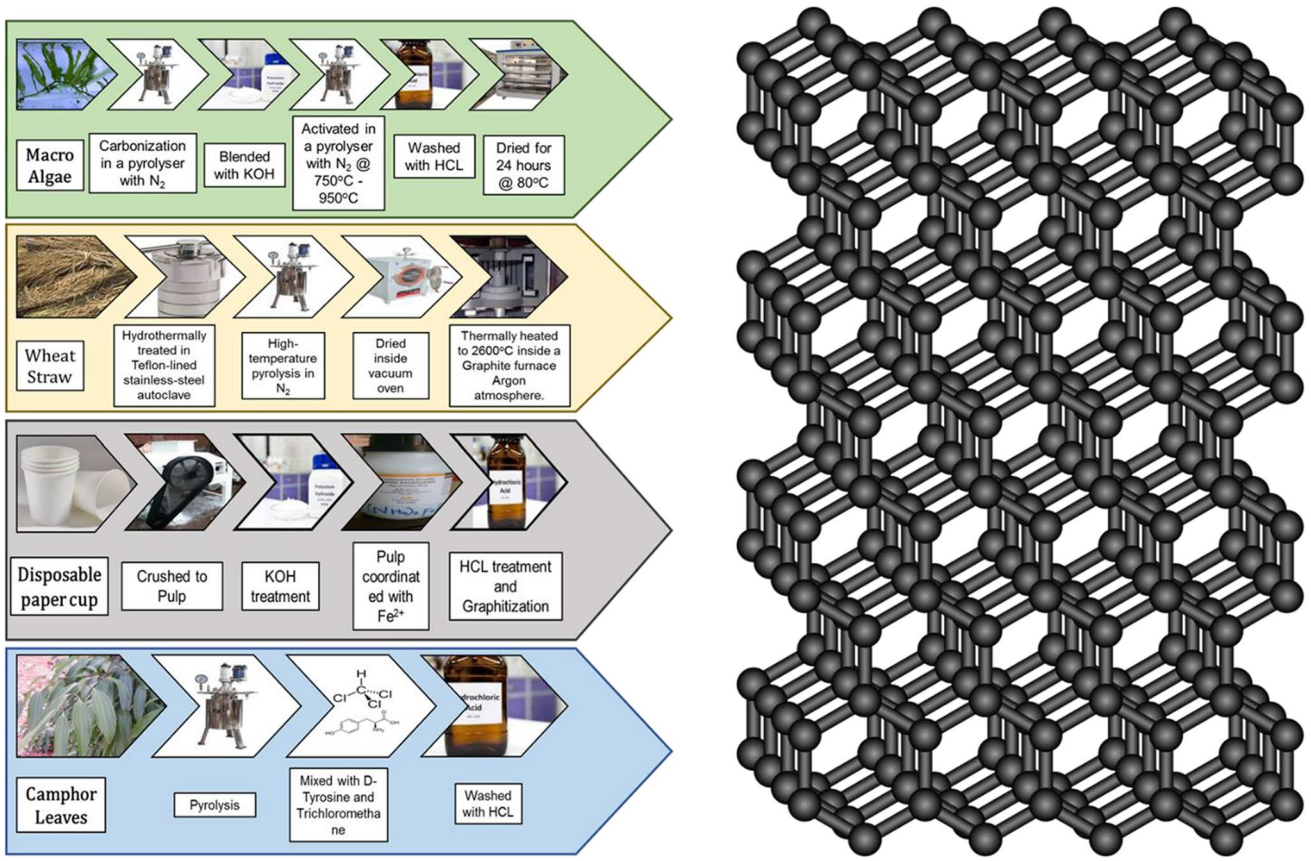

Fig. 6 Different process pathways for fabrication of pristine FLG from natural precursors

as a reducing agent formed corrugated-edged graphene nanosheets (GN). GNs developed have been used in supercapacitors and dye-sensitized solar cells. The same substrate has favorable surface characteristics (about 0.91 I_D/I_G, and nearly 0.4-nm sheet thickness) for direct air CO_2 adsorption operation (Pandey et al. 2021). Recently, *Hibiscus sabdariffa* sticks have been carbonized, KOH activated, and pyrolyzed to produce porous graphene-like carbon sheets with a high specific surface area of about 2300m^2g^{-1} (BET), and a high pore volume of 1.3 $cm^3\ g^{-1}$, with 2.2-nm average pore size (Nanaji et al. 2021). The sheets with high energy and power density (21.37 Wh kg^{-1} and 13,420 W kg^{-1}) are suited for electrode development and can have CO_2 capture potential. Cellulose filter paper engraved using laser produces laser-induced graphene (LIG) which has a sheet resistance of 71.6 Ω/square and nearly 1 I_D/I_G (Raman). LIG derived from laser induction exhibits strain and bending functionality (Kulyk et al. 2021), and LIG may be modified for carrying out CO_2 adsorption studies.

A different route was investigated by Alkhavan, Bijanzad, and Mirsepah, making use of general wastes from day-to-day life, including natural waste like wood, leaf, bone, and cow dung, and also regular human activity-based waste, namely, bagasse, and newspaper. These were converted into GO and rGO suspensions. The route involved the production of industrial soot, by imperfect burning over a period of 5 days to obtain powdered soot which is carbonized by heating at 450 °C for 24 h; the as-prepared material was mixed with ferric chloride hexahydrate in distilled water along with continuous stirring. The graphitized material was then converted to GO using the modified Hummers' method. The obtained GO was then reduced by hydrazine reduction to get graphene (Fig. 7). Although this method is extensive and makes use of Hummer's method, it produces high-quality GO suspensions, which may be co-dispersed with polymer nanoparticles to yield graphene sheets. This method avoids the segregation of wastes and leads to a consistent final product. The properties of the obtained rGO sheets are independent of the carbon source and the properties observed, especially the I_D/I_G ratios are comparable to rGO sheets obtained from industrial graphite (Akhavan et al. 2014). Another production route of rGO utilizing waste dry cell batteries, a known persistent environmental hazard, involves utilization of graphite powder obtained from zinc-carbon dry cell electrodes. Improved Hummer's method has been used to obtain GO, which undergoes hydrazine

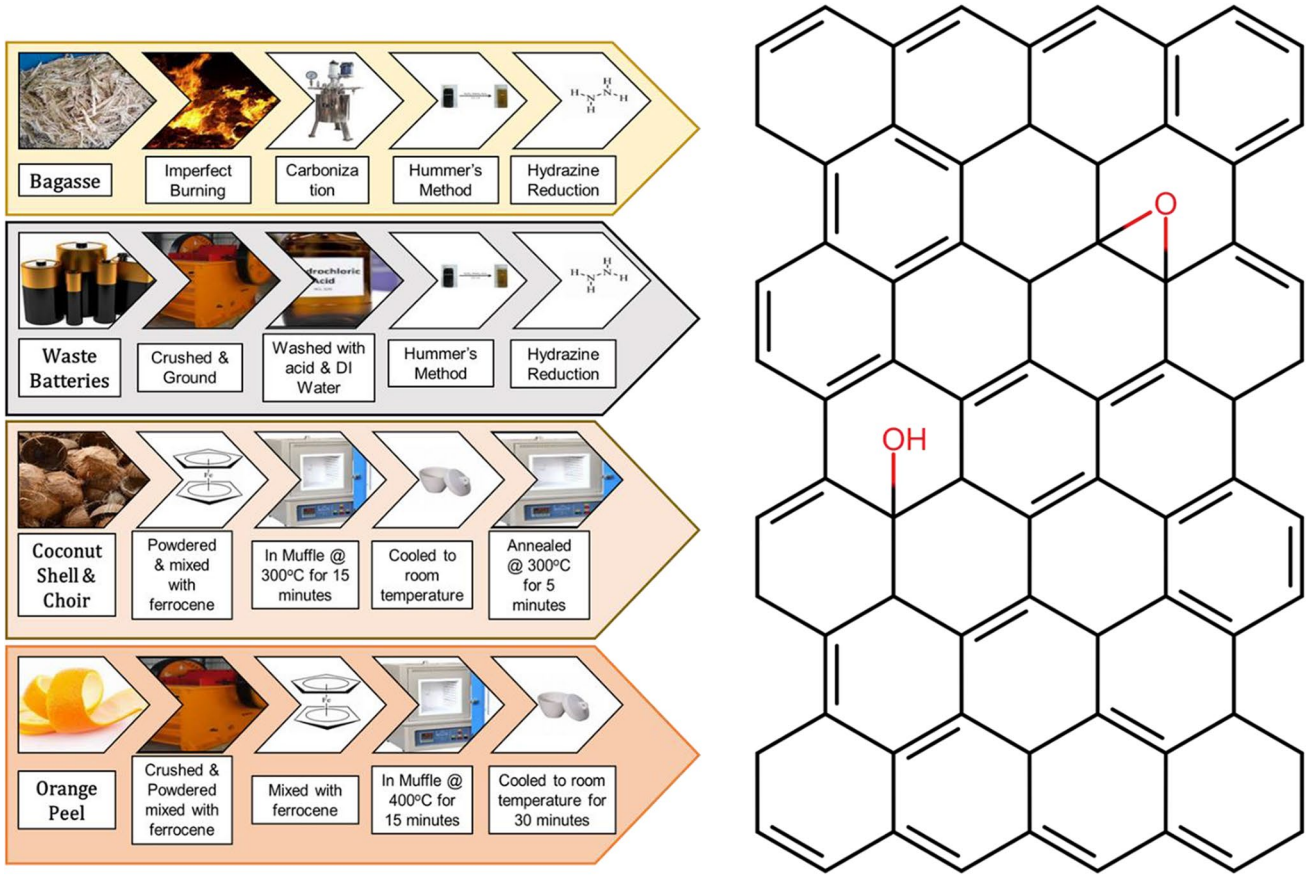

Fig. 7 Different process pathways for fabrication of RGO from natural precursors

reduction to yield rGO (Fig. 7). A stable anionic (Zeta potential of -23.5 ± 0.41 mV) dispersion is obtained upon dispersing the rGO obtained in an aqueous medium, and the rGO has high conductivity due to restoration of sp^2 hybridization indicated by the elimination of diffraction peak at 11.54° in XRD analysis and a reduction in the interlayer distance from 0.765 to 0.361 nm; the I_D/I_G ratios obtained are comparable to values observed for rGO obtained from industrially sourced graphite, so air/CO_2 capture potential may be tested for graphene derivatives obtained via this route (Roy et al. 2016). Agricultural waste, namely, coconut shell and coconut choir, can also yield high-quality rGO by catalytic oxidation. This requires the carbonization of coconut shell and choir (crushed and ground to a fine powder), while mixed with ferrocene in a 1:5 ratio inside a muffle furnace for 15 min at 300 °C under atmospheric conditions. The mixture is then cooled to room temperature, which gives GO. This GO was thermally annealed for an additional 5 min, which is sufficient to get rGO from GO (Fig. 7). The final product obtained was a 2D rGO sheet with a well-graphitized structure, which was thin and consisted of a few layers indicated by SEM and AFM. Higher interlayer spacing for both choir and shell samples was attributed to minute quantities of residual functional groups mostly containing oxygen bonds. Zeta potential tests carried out indicated anionic dispersion stable in aqueous media (Tamilselvi et al. 2020). High-quality rGO may be synthesized efficiently, economically, and rapidly using this method. The CO_2/air adsorption capability has not been tested; however, these rGO sheets were tested to be used as high-performance, flexible supercapacitors. Similarly, agro-wastes in both individual and tri composite forms, namely, rice bran, sugarcane bagasse, and orange peel were dried, crushed, and powdered to act as carbon precursors. They were mixed with ferrocene in a 1:3 ratio and introduced to the muffle furnace at 400 °C. The black solid residues were kept at ambient conditions for 30 min to obtain the final product. GO was effectively synthesized using relatively low temperatures (Hashmi et al. 2020). There were no tests carried out to air adoption capabilities, but it sheds light on a less arduous method to arrive at GO. Rice husk biomass may be used as a carbon precursor. Rice husk (after being washed) was treated inside a tube furnace for 2 h with N_2 blanketing at 700 °C. The ash was treated with NaOH at 900 °C for 2 h under a protective atmosphere. The product, upon mixing with de-ionized (DI) water, yielded a mixture of carbon from

rice husk (RHC) and silica. The carbon sourced from rice husk was obtained by vacuum filtration, and the same was treated with H_2SO_4, ultrasonicated for 5 h, and mixed with nitric acid. Then, it was vacuum filtered, thoroughly washed, pH adjusted, and autoclaved at 200 °C for 10 h. The sample was filtered to rice husk quantum dots (RHQD) (Wang et al. 2016). The intended product of graphene and graphene derivatives may be obtained by using KOH instead of NaOH and then using HCl to get GO. The same may be converted to rGO by suitable reduction methods. A readily available waste source, oil palm biomass, has been pulped, separated, and carbonized to derive lignin-derived graphene oxide powder (LGO). LGO obtained exhibits surface characteristics of 280.1 $m^2\ g^{-1}$(BET) microporous area, 0.222 $cm^3\ g^{-1}$ pore volume, and pore size of 3.15 nm (Yaqoob et al. 2021). High current density (15.65 mAm^{-2}) and heavy metal removal (83.5% removal of cadmium) are observed in microbial fuel cells using lignin-based graphene oxide (LGO) anodes. The improved surface may be tested as CO_2 adsorbent. Fairly abundant *Miscanthus* grass has been pyrolyzed, edge carboxylated, and ultrasonically exfoliated to yield graphene oxide and graphene quantum dots (Yan et al. 2021). The single-step method produces various graphene derivatives with controllable proportions.

A pathway to carbon sheets doped with nitrogen (known to improve gas-sieving characteristics (Li et al. 2017) without the GO intermediary incorporated the mixing of dried and crushed bagasse with melamine (an inexpensive chemical) in varying weight ratios inside a Teflon-lined autoclave. The product obtained was heated to 850 °C for 3 h in an argon atmosphere to facilitate N-doping. The result obtained is N-doped carbon sheets like graphene. The final product, the N-doped carbon sheets, from AFM established layered carbon structures similar to graphene. The N-doped carbon sheets were tested for sulfur retention in Li–S batteries. This route does not involve Hummers' method (Babu and Ramesha 2019). Testing for the CO_2 adsorption capacity may yield favorable results as a sheet-like structure is confirmed through SEM analysis. Coal tar pitch dispersed in ethyl acetate and carbonized with expanded vermiculite to yield carbon nanosheets (CNS) which show high specific surface area (280.1 $m^2\ g^{-1}$(BET)) and high pore volume (0.222 $cm^3\ g^{-1}$). CNSs demonstrate excellent performance as an anode in lithium-ion batteries (623 $mAhg^{-1}$ (2 Ag^{-1})) reversible capacity with 99.7% capacity retention after 200 cycles) and may have good CO_2 removal potential (Wang et al. 2021).

Graphene aerogel may be obtained from microcrystalline nanocellulose which involves the development of cellulose aerogel composited with a phenolic resin, and then subsequent carbonization in nitrogen at 600 °C to obtain graphene aerogel. This provided a high yield of products of about 48% with a specific porous network. BET analysis reveals a specific area of about 1426.11 m^2/g, indicating a prospective candidate for adsorption applications (Li et al. 2020a, b). The use of phenol is a safety issue in this process, and microcrystalline cellulose, based on organic precursors, requires an extensive production route. Date syrup processed through heating, KCl treatment, sequential vacuum heating (N_2), and HCl washing yields 3D networked graphene foam which exhibits a specific surface area of about $650 m^2 g^{-1}$(BET), ~ 0.4 $cm^3\ g^{-1}$ pore volume, and average particle size of 6 nm (Abed et al. 2023). Potential applications are yet to be investigated, with CO_2 adsorption studies being one of them. Waxed cork has been treated with CO_2 and Nd:YAG fiber lasers to create three-dimensional laser-induced graphene (LIG) network (Silvestre et al. 2022). Wax-based ink pre-treatment of cork eliminates the need for mechanical supports. Three-dimensional porous LIG has the potential for unsupported CO_2 capture devices.

Waste chicken fat can be used to yield unified monolayer graphene film, utilizing low-pressure carbon vapor deposition (LPCVD) on Cu substrate. Chicken oil was obtained from waste chicken by the dry rendering process. Electrochemical delamination was used to transfer graphene onto a substrate polymethylmethacrylate (PMMA) to form PMMA/graphene composite, and finally, acetone was used to eliminate PMMA. The transferred graphene is continuous with no patches, Raman spectroscopy indicated a value of $I_D/I_G < 0.1$ and $I_{2D}/I_G > 3$, indicating uniform coverage of high-quality monolayer graphene. The hexagonal diffraction pattern indicated a mostly crystalline area (Rosmi et al. 2016). The requirement of a CVD setup restricts large-scale production potential at the moment. A similar method illustrated a route to directly obtain a single uniform layer of pristine graphene of high quality, with minimal defects and 97% transparency. The process involved spin coating of carbon source onto PMMA, and then subsequent CVD onto a Cu film, with an operating temperature of 800–1100 °C with reductive gas flow and low-pressure conditions. UV–Vis's analysis points to typical $\pi > \pi$ transition for aromatic C–C bonds in graphene film (peaks at 268 nm) and formation of monolayer graphene (peaks at 550 nm) (Ruan et al. 2011). A similar method involved CVD to obtain patterned graphene electrodes from quinone diluted coal tar pitch coated on a silica substrate, baked at 240 °C. Thermal annealing of the sample was carried out by CVD post deposition of nickel layer. Upon cooling, $FeCl_3$ solution was used to etch away the Ni layer. UPS (ultraviolet photoelectron spectroscopy) to measure the work function of the prepared electrode showed a hole injection barrier of 0.43 eV. Extended characterization methods may be carried out to further analyze the morphological characteristics of prepared graphene samples (Seo et al. 2015). Gas adsorption experiments may also be carried out. The work of Cui et al. (2017) showed the production of high-quality graphene foil (GF) from regular plastic wastes

on a large scale via a solid-state chemical vapor deposition method. The method claims to be safe, simple, and cheap. The GF demonstrates higher electrical conductivity (beyond 3500 Scm^{-1}) than that of the conventional free-standing graphene films which require very high–temperature graphite reactors for synthesis. The GF demonstrates stable electrochemical duty as an electrode inside a foldable Li-ion battery demonstrating structural flexibility and consistent electrochemical performance. It is also able to generate beyond 300 °C against an applied potential difference of 5 V when operated as a heating element. Hence, the GF synthesized is extremely versatile and opens up numerous avenues for the implementation and application of waste-sourced graphene. Raman spectra indicate negligible structural defects and also establish exceptional degrees of graphitization and crystallinity (narrow and intense G-band), and crystallinity is also inferred from XRD analysis (26.7° sharp peak) while EDS reconfirms high graphitization. GFs prepared remain structurally consistent irrespective of the precursors utilized, and testing these versatile devices for CO_2 adsorption may yield interesting insights.

Graphite rods from empty mosquito repellent refills, another common waste from households, were shown to be a viable source for obtaining graphene in an oxidation state, with carbon atoms in various functional groups. The method involves electrochemical exfoliation followed by treatment with sodium citrate to reduce the oxidation state. Before electrochemical exfoliation, the graphite rods have to be removed and washed with dilute HCL and also boiled to remove impurities. The product obtained remains untested for any real-life applications in this synthesis-focused work (Udhaya Sankar et al. 2018). Another common waste product similar to graphite rods from mosquito repellent refills is pencil cores, which tend to be discarded before complete utilization. The method utilized electrochemical exfoliation to turn the same pencil cores to high-quality graphene oxide flakes. The electrochemical approach was green, and cost effective, involving aqueous electrolytes H_2SO_4/H_3PO_4. TEM analysis indicated a few stacked layers with wrinkled morphology. SEM images showed GO flakes to be about 1–5 microns. FTIR results showed the presence of oxygen functionalization at the surface (Liu et al. 2013). This method is comparatively primitive, as compared to methods that form more stacked layers, and no tests were carried out to check gas adsorption performance. Both, waste dry cell battery and pencil cores, have undergone electrochemical exfoliation and thermal treatment to yield reduced graphene oxide modified with citric acid (CrGO) that has a crystallite size of about 17 nm and surface roughness of about 0.5 nm (Singh et al. 2023). CO_2 adsorption applications may be investigated for CrGO.

A major waste material from the sugar and juice industry is pectin-rich mango peels. They have been used as raw material to synthesize graphene using a plasma-enhanced CVD technique. This enhanced CVD route has been able to synthesize both monolayer and multilayer graphene. The number of layers deposited on the substrate is controlled by the plasma exposure time, sheet thickness of graphene being inversely proportional to the time of plasma treatment (an hour of plasma treatment yields pristine single layer graphene). The etching effect of plasma, an apparent process drawback, may be harnessed to directly obtain graphene with vacancy defects, a very effective CO_2 adsorbent (Shah et al. 2018). However, gas adsorption performance has not been investigated (Fig. 8).

The most abundant and easily available waste material is PET mineral water bottles. El Essawy et al. (2017) devised a way of synthesizing graphene by crushing and sieving waste PET bottles into desired size (1–3 mm) and then treating it in an autoclave reactor. XRD analysis of the sample displayed broad diffraction peaks corresponding to (002), (100), and (101) reflections. The broad (002) peak indicated inter-layer distances which were larger than crystalline graphite. The presence of a (101) peak suggests a stacking of layers in the resulting samples (Shen and Lua 2013). Though the prepared sample was not tested for CO_2 adsorption, methylene blue (MB) and acid blue 25 (AB25) adsorptions were investigated to optimize adsorbent dosages and contact time using response surface methodology. A relatively cheap and simple utilization of waste plastic bottle carbon precursor has also been studied by Kamali et al. (2019) where they

Fig. 8 Various natural precursors for pristine single-layer graphene fabrication using CVD

used a molten salt strategy for converting plastic bottles into a highly conductive nanostructured carbon. Small pieces of plastic waste and sodium chloride were heated to 1300 °C at a ramp of 10 °C/min and then quenched, in an alumina crucible inside a resistance furnace. The salt was dissolved out of the product to obtain synthesized amorphous carbon consisting of crystalline graphitic nanosheets of less than 10-nm thickness. Advincula et al. (2023) worked on using shredded consumer waste plastic and metallurgical coke as a precursor to yield turbostratic flash graphene (TFG). The product was achieved through flash joule heating (FJH), a pre-flashed blend of 5% carbon back and shredded high-density polyethylene (HDPE) at 120 V for 500 ms (Algozeeb et al. 2020). Metallurgical coke flash graphene (MCFG) was prepared by FJH pulse at varying duty cycles at 1 kHz frequency. The process yields of PFG and MCFG were about 40% and 95% respectively. After FJH, the average I_{2D}/I_G ratios for WPFG and MCFG indicated quality. The production process required 99% less water, 98% less energy, and 98.8% reduced gas emissions compared to the conventional production routes for graphene. FJH as a method for FG is an easy and affordable synthesis route that may be used on a large scale. Huang et al. (2021) have worked on developing carbon nanotubes (CNTs) from waste polyethylene by mixing it with a prescribed amount of ethanol, cobalt (II) hexahydrate under vigorous stirring with a protectant; and varying reactant precursors supported with varying amounts of cobalt nitrate at elevated temperatures. CNT yield using oleyl amine protectant was the highest (59%). A high yield of CNTs, with a length of 5–10 µm, and a diameter of less than 50 nm, was confirmed from SEM images. Similar to the study on waste PET bottles by Essawy et al., CNTs were tested for the adsorption of methylene blue, where it exhibited high adsorption capacity (up to 107.1 mg g^{-1}). BET concluded a very high specific area of 195.7 m^2 g^{-1} that may be tested as an effective CO_2 adsorbent.

Investigation of works that have employed the bottoms-up route indicates that bulk production of graphene and its derivatives is viable and can be categorized broadly into 4 categories as depicted in Fig. 9. Most notably, abundantly available carbon precursors in the form of self-sustaining biomass, organic wastes, and domestic plastic waste have the potential to reduce the price involving industrial grade precursors. Work involving the production of rGO from sources such as agricultural wastes (rice husk, coconut husk, bagasse) has the least temperature requirement during synthesis; however, ferrocene used during carbonization might increase the overall cost. A major advantage of using ferrocene not only reduces the temperature requirement but also reduces the required time which in turn compensates for the cost of ferrocene. The produced rGO has also exhibited comparable properties to derivatives obtained from industrial graphite. Further investigation will help to identify better

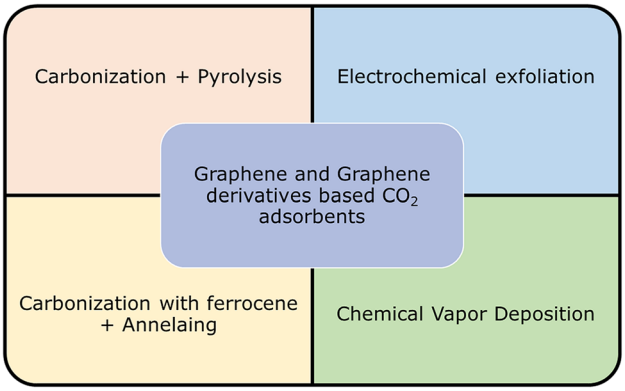

Fig. 9 Viable fabrication routes for naturally sourced graphene-based CO_2 adsorbents

precursors for this route. The produced rGO can be tested for its CO_2 capture capacity, with a promising potential for developing sustainable CO_2 adsorbents with high surface area. Although the precursor cost goes down when using natural sources, certain raw materials, namely, waste dry cell batteries, require the Hummer's method to obtain GO as an intermediary step and later hydrazine reduction to get rGO, increasing overall process cost.

CVD has also been demonstrated as a pathway to very high–quality, pristine graphene sheets from various natural resources (Fig. 8), which may be impinged (to introduce defects) and doped (with metals) to obtain high-performing CO_2 adsorbents. The price reduction achieved by sourcing an easily available raw material is offset by the cost and low yield involved in the CVD process. Production in bulk is still a major challenge in this route. This route is however just a breakthrough in the CVD process away from becoming an extremely efficient route to high-quality graphene.

Among all the processes considered, a few layers of graphene obtained via the chemical treatment of carbonized products of natural and waste-based carbon precursors is the most interesting process. The utilization of macro-algae highlights a pathway to graphene-based CO_2 adsorbents with minimal cost requirements. Wheat straw, paper cups, and camphor leaves indicate obstacles to economic feasibility due to the necessity of graphite reactor, ammonium iron(II) sulfate, and D-tyrosine, respectively. However, graphene obtained from macro-algae using KOH activation followed by pyrolysis not only reduces the cost of the source but also energy decreases the energy requirement of the process. It has demonstrated notable CO_2 adsorption capacity and may be improved further by incorporating functional groups on the prepared adsorbents. It may also be viable to treat other carbon precursors in the same manner and analyze the final products obtained for their CO_2 capture performance. The pyrolysis temperature requirement of 850 °C is a minor trade-off for the results demonstrated.

Conclusion

Multiple instances of investigations, i.e., experimental work, have been carried out to test the CO_2 adsorption capacity of graphene and its derivatives. Graphene and its derivatives sourced from the top-down route involving industrial grade precursors have shown exceptional CO_2 adsorption performance due to favorable surface characteristics as an adsorbent. Functionalization has been accomplished to improve the capability of graphene as an adsorbent. Certain innovations have also been achieved, notably the establishment of free-standing graphene-based membranes eliminating the need for a template. However, irrespective of the advancements, the requirement of highly pure precursors and an extensive list of chemicals involved in this route pose a major demerit on the aspect of utilizing graphene as a universally accepted direct air capture adsorbent for CO_2. The environmental consequences from a life cycle assessment approach create doubt about the viability and environmental compatibility of graphene and graphene-based derivatives. But this hurdle may be overcome by synthesizing such adsorbents from naturally sourced and waste-based carbon precursors. Certain works have already highlighted the use of naturally sourced graphene as an effective air adsorbent. More investigations must be carried out to test for the viability of graphene from an increased pool of carbon precursors. Graphene development from waste plastics and naturally occurring sources have seen a large volume of work, yet very few of such developed graphene and derivatives have been tested for CO_2 adsorption behavior. Graphene has a wide range of applications including its capability as a viable supercapacitor, an excellent pollutant capture capability, and even geo-sensor properties, and it is necessary to test all its capabilities. Yet, the need to devote a substantial number of resources and time to develop and test direct air capture systems for CO_2 adsorption based on graphene and graphene derivatives from natural and waste carbon precursors is urgent and global.

Acknowledgements SC wishes to acknowledge AICTE for a doctorate fellowship.

Author contribution All authors contributed to the study conception and design. Material preparation, data collection, and analysis were performed by Saswata Chakraborty and Ranadip Saha. The first draft of the manuscript was written by Saswata Chakraborty and Ranadip Saha. Sudeshna Saha critically reviewed the first draft, made necessary corrections and improvement, and supervised the whole work. All authors read and approved the final manuscript.

Funding This work was supported by the Department of Science and Technology-Science and Engineering Research Board (DST-SERB) for funding [EEQ/2016/000702]. Author S.C. received a research scholarship from AICTE, India.

Declarations

Competing interests The authors declare no competing interests.

References

Abed M et al (2023) From date syrup to three-dimensional graphene network. Phys Scr 98(8). https://doi.org/10.1088/1402-4896/ace3fe

Advincula PA et al (2023) Waste plastic- and coke-derived flash graphene as lubricant additives. Carbon 203(October 2022):876–885. https://doi.org/10.1016/j.carbon.2022.12.035

Aguilar JCS et al (2021) Hydroxyl-functionalized graphene from spent batteries as efficient adsorbent for amoxicillin. Chem Eng Trans 86:331–336. https://doi.org/10.3303/CET2186056

Ai N et al (2021) Facile synthesis of macroalgae-derived graphene adsorbents for efficient CO2 capture. Process Saf Environ Prot 148:1048–1059. https://doi.org/10.1016/j.psep.2021.02.014

Akhavan O et al (2014) Synthesis of graphene from natural and industrial carbonaceous wastes. RSC Adv 4(39):20441–20448. https://doi.org/10.1039/c4ra01550a

Alghamdi AA et al (2018) Enhanced CO2 adsorption by nitrogen-doped graphene oxide sheets (N-GOs) prepared by employing polymeric precursors. Materials 11(4). https://doi.org/10.3390/ma11040578

Algozeeb WA et al (2020) Flash graphene from plastic waste. ACS Nano 14(11):15595–15604. https://doi.org/10.1021/acsnano.0c06328

Ali A et al (2019) Graphene-based membranes for CO2 separation. *Materials Science for Energy Technologies*. KeAi Communications Co., 83–88. https://doi.org/10.1016/j.mset.2018.11.002

Armano A, Agnello S (2019) Two-dimensional carbon: a review of synthesis methods, and electronic, optical, and vibrational properties of single-layer graphene. C — J Carbon Res 5(4):67. https://doi.org/10.3390/c5040067

Baachaoui S et al (2021) Density functional theory investigation of graphene functionalization with activated carbenes and its application in the sensing of heavy metallic cations. J Phys Chem C 125(48):26418–26428. https://doi.org/10.1021/acs.jpcc.1c07247

Babu DB, Ramesha K (2019) Melamine assisted liquid exfoliation approach for the synthesis of nitrogen doped graphene-like carbon nano sheets from bio-waste bagasse material and its application signi high areal density Li-S batteries. Carbon 144:582–590. https://doi.org/10.1016/j.carbon.2018.12.101

Balasubramanian R, Chowdhury S (2015) Recent advances and progress in the development of graphene-based adsorbents for CO2 capture. J Mater Chem A. Royal Soc Chem 21968–21989. https://doi.org/10.1039/c5ta04822b

Bermeo M et al (2022) Critical assessment of the performance of next-generation carbon-based adsorbents for CO2 capture focused on their structural properties. Sci Total Environ 810:151720. https://doi.org/10.1016/j.scitotenv.2021.151720

Bhanja P et al (2016) Functionalized graphene oxide as an efficient adsorbent for CO2 capture and support for heterogeneous catalysis. RSC Adv 6(76):72055–72068. https://doi.org/10.1039/c6ra13590k

Cabrera-Sanfelix P (2009) Adsorption and reactivity of CO2 on defective graphene sheets. J Phys Chem A 113(2):493–498. https://doi.org/10.1021/jp807087y

IPCC (2005) IPCC Special Report on Carbon Dioxide Capture and Storage. Prepared by Working Group III of the Intergovernmental Panel on Climate Change. In: Metz B, Davidson O, de

Coninck HC, Loos M, Meyer LA (eds) Cambridge University Press, Cambridge, United Kingdom and New York, NY, USA, p 442

Castro-Muñoz R et al (2022) A new relevant membrane application: CO2 direct air capture (DAC). Chem Eng J 446(March). https://doi.org/10.1016/j.cej.2022.137047

Chakraborti H, Pal SK (2014) Assessment of amine functionalized graphene nanoflakes for anode materials in Li-ion batteries: an ab initio study. Chem Phys Lett 600:118–122. https://doi.org/10.1016/j.cplett.2014.03.065

Chandra V et al (2012) Highly selective CO2 capture on N-doped carbon produced by chemical activation of polypyrrole functionalized graphene sheets. Chem Commun 48(5):735–737. https://doi.org/10.1039/c1cc15599g

Chen F et al (2016) Facile synthesis of few-layer graphene from biomass waste and its application in lithium ion batteries. J Electroanal Chem 768:18–26. https://doi.org/10.1016/j.jelechem.2016.02.035

Chen H et al (2021) The synergistic effects of surface functional groups and pore sizes on CO2 adsorption by GCMC and DFT simulations. Chem Eng J 415(February):128824. https://doi.org/10.1016/j.cej.2021.128824

Chowdhury S, Balasubramanian R (2016) Highly efficient, rapid and selective CO2 capture by thermally treated graphene nanosheets. J CO2 Utilization 13:50–60. https://doi.org/10.1016/j.jcou.2015.12.001

Chuah CY et al (2021) Carbon molecular sieve membranes comprising graphene oxides and porous carbon for co2/n2 separation. Membranes 11(4). https://doi.org/10.3390/membranes11040284

Chui S-Y et al (1999) A chemically functionalizable nanoporous material [Cu $_3$ (TMA) $_2$ (H $_2$ O) $_3$] *n*. Available at: https://doi.org/10.1126/science.283.5405.1148

Coello-Fiallos D et al (2017) DFT comparison of structural and electronic properties of graphene and germanene: monolayer and bilayer systems. https://doi.org/10.1016/j.matpr.2017.07.011

Cui L et al (2017) Trash to treasure: converting plastic waste into a useful graphene foil. Nanoscale 9(26):9089–9094. https://doi.org/10.1039/c7nr03580b

El Essawy NA et al (2017) Green synthesis of graphene from recycled PET bottle wastes for use in the adsorption of dyes in aqueous solution. Ecotoxicol Environ Saf 145(April):57–68. https://doi.org/10.1016/j.ecoenv.2017.07.014

Esrafili MD (2019) Electric field assisted activation of CO2 over P-doped graphene: a DFT study. J Mol Graph Model 90:192–198. https://doi.org/10.1016/j.jmgm.2019.05.008

Fatihah N et al (2019) Preparation and characterization of APTES-functionalized graphene oxide for CO 2 adsorption effect of intermediate layer on gas separation performance of disk supported carbon membrane view project polymeric membranes: fabrication and characterization view project preparation and characterization of APTES-functionalized graphene oxide for CO 2 adsorption. J Adv Res Fluid Mech Therm Sci J Homepage 61:297–305. https://doi.org/10.13140/RG.2.2.10612.30085

Fauth DJ et al (2012) Investigation of porous silica supported mixed-amine sorbents for post-combustion CO 2 capture. Energy Fuels 26(4):2483–2496. https://doi.org/10.1021/ef201578a

Fraga TJM et al (2019) Functionalized graphene-based materials as innovative adsorbents of organic pollutants: a concise overview. Braz J Chem Eng 36(1):1–31. https://doi.org/10.1590/0104-6632.20190361s20180283

Fujita JI et al (2017) Near room temperature chemical vapor deposition of graphene with diluted methane and molten gallium catalyst. Sci Rep 7(1). https://doi.org/10.1038/s41598-017-12380-w

Gao X et al (2022) Carbonaceous materials as adsorbents for CO2 capture: synthesis and modification. Carbon Capture Sci Technol 3(December 2021):100039

Garcia-Gallastegui A et al (2012) Graphene oxide as support for layered double hydroxides: enhancing the CO2 adsorption capacity. Chem Mater 24(23):4531–4539. https://doi.org/10.1021/cm3018264

Gunawardene OHP et al (2022) Carbon dioxide capture through physical and chemical adsorption using porous carbon materials: a review. Atmosphere. https://doi.org/10.3390/atmos13030397

Gupta RK et al (2017) Aminoazobenzene and diaminoazobenzene functionalized graphene oxides as novel class of corrosion inhibitors for mild steel: experimental and DFT studies. Mater Chem Phys 198:360–373. https://doi.org/10.1016/j.matchemphys.2017.06.030

Hashmi A et al (2020) Muffle atmosphere promoted fabrication of graphene oxide nanoparticle by agricultural waste. Fuller, Nanotubes, Carbon Nanostruct 28(8):627–636. https://doi.org/10.1080/1536383X.2020.1728744

Hsu KJ et al (2021) Multipulsed millisecond ozone gasification for predictable tuning of nucleation and nucleation-decoupled nanopore expansion in graphene for carbon capture. ACS Nano 15(8):13230–13239. https://doi.org/10.1021/acsnano.1c02927

Huang Z et al (2021) High-yield production of carbon nanotubes from waste polyethylene and fabrication of graphene-carbon nanotube aerogels with excellent adsorption capacity. J Mater Sci Technol 94:90–98. https://doi.org/10.1016/j.jmst.2021.02.067

Huang L, Jia W, Lin H (2020) Etching and acidifying graphene oxide membranes to increase gas permeance while retaining molecular sieving ability. AIChE J 66(12). https://doi.org/10.1002/aic.17022

Hummers WS, Offeman RE (1958) Preparation of graphitic oxide. Available at: https://doi.org/10.1021/ja01539a017

Jiříčková A et al (2022) Synthesis and applications of graphene oxide. Materials MDPI. https://doi.org/10.3390/ma15030920

Kamali AR et al (2019) Molten salt conversion of polyethylene terephthalate waste into graphene nanostructures with high surface area and ultra-high electrical conductivity. Appl Surf Sci 476(January):539–551. https://doi.org/10.1016/j.apsusc.2019.01.119

Kamel M et al (2020) Theoretical elucidation of the amino acid interaction with graphene and functionalized graphene nanosheets: insights from DFT calculation and MD simulation. Amino Acids 52(10):1465–1478. https://doi.org/10.1007/s00726-020-02905-5

Kárászová M et al (2020) Post-combustion carbon capture by membrane separation, review. Sep Purif Technol. Elsevier B.V. https://doi.org/10.1016/j.seppur.2019.116448.

Kulyk B et al (2021) Laser-induced graphene from paper for mechanical sensing. ACS Appl Mater Interfaces 13(8):10210–10221. https://doi.org/10.1021/acsami.0c20270

Kumar R et al (2014) Porous graphene frameworks pillared by organic linkers with tunable surface area and gas storage properties. Chem Commun 50(16):2015–2017. https://doi.org/10.1039/c3cc46907g

Lee S-Y, Park S-J (2012) Comprehensive review on synthesis and adsorption behaviors of graphene-based materials. Carbon Lett 13(2):73–87. https://doi.org/10.5714/cl.2012.13.2.073

Li W et al (2016) Highly selective CO 2 adsorption of ZnO based N-doped reduced graphene oxide porous nanomaterial. Appl Surf Sci 360:143–147. https://doi.org/10.1016/j.apsusc.2015.10.212

Li J et al (2017) Enhanced CO 2 capture on graphene via N, S dual-doping. Appl Surf Sci 399:420–425. https://doi.org/10.1016/j.apsusc.2016.11.157

Li J et al (2020a) A novel graphene aerogel synthesized from cellulose with high performance for removing MB in water. J Mater Sci Technol 41:68–75. https://doi.org/10.1016/j.jmst.2019.09.019

Li J et al (2020b) Insights into the adsorption/desorption of CO2 and CO on single-atom Fe-nitrogen-graphene catalyst under electrochemical environment. J Energy Chem 53:20–25. https://doi.org/10.1016/j.jechem.2020.04.016

Lin Y et al (2013) Bulk preparation of holey graphene via controlled catalytic oxidation. Nanoscale 5(17):7814–7824. https://doi.org/10.1039/c3nr02135a

Liu J et al (2013) A green approach to the synthesis of high-quality graphene oxide flakes via electrochemical exfoliation of pencil core. RSC Adv 3(29):11745–11750. https://doi.org/10.1039/c3ra41366g

Liu H et al (2015) Selectivity trend of gas separation through nanoporous graphene. J Solid State Chem 224:2–6. https://doi.org/10.1016/j.jssc.2014.01.030

Liu Y et al (2019) Ultrasound-assisted amine functionalized graphene oxide for enhanced CO2 adsorption. Fuel 247:10–18. https://doi.org/10.1016/j.fuel.2019.03.011

Lyu W et al (2022) Nitrogen atom-doped layered graphene for high-performance CO2 /N2 adsorption and separation. Energies 15(10). https://doi.org/10.3390/en15103713

Malekian F et al (2019) Recent progress in gas separation using functionalized graphene nanopores and nanoporous graphene oxide membranes. Springer Verlag, European Physical Journal Plus. https://doi.org/10.1140/epjp/i2019-12612-4

Markewitz P et al (2012) Worldwide innovations in the development of carbon capture technologies and the utilization of CO2. Energy Environ Sci 5(6):7281–7305. https://doi.org/10.1039/c2ee03403d

Meconi GM, Zangi R (2020) Adsorption-induced clustering of CO2on graphene. Phys Chem Chem Phys 22(37):21031–21041. https://doi.org/10.1039/d0cp03482g

Mensah K et al (2022) Novel nano-ferromagnetic activated graphene adsorbent extracted from waste for dye decolonization. J Water Process Eng 45(December 2021):102512. https://doi.org/10.1016/j.jwpe.2021.102512

Mino L et al (2014) CO2 capture by TiO2 anatase surfaces: a combined DFT and FTIR study. J Phys Chem C 118(43):25016–25026. https://doi.org/10.1021/jp507443k

Mishra AK, Ramaprabhu S (2012) Nanostructured polyaniline decorated graphene sheets for reversible CO 2 capture. J Mater Chem 22(9):3708–3712. https://doi.org/10.1039/c2jm15385h

Mofidi F, Reisi-Vanani A (2020) Investigation of the electronic and structural properties of graphyne oxide toward CO, CO2 and NH3 adsorption: a DFT and MD study. Appl Surf Sci 507(June 2019). https://doi.org/10.1016/j.apsusc.2019.145134

Mohamed HH, Alsanea AA (2020) TiO2/carbon dots decorated reduced graphene oxide composites from waste car bumper and TiO2 nanoparticles for photocatalytic applications. Arab J Chem 13(1):3082–3091. https://doi.org/10.1016/j.arabjc.2018.08.016

Nanaji K et al (2021) A novel approach to synthesize porous graphene sheets by exploring KOH as pore inducing agent as well as a catalyst for supercapacitors with ultra-fast rate capability. Renew Energy 172:502–513. https://doi.org/10.1016/j.renene.2021.03.039

Nemitallah MA et al (2017) Oxy-fuel combustion technology: current status, applications, and trends. Int J Energy Res. John Wiley and Sons Ltd, pp. 1670–1708. https://doi.org/10.1002/er.3722

Nikolopoulos N et al (2011) Numerical investigation of the oxy-fuel combustion in large scale boilers adopting the ECO-Scrub technology. Fuel 90(1):198–214. https://doi.org/10.1016/j.fuel.2010.08.007

Nwaoha C et al (2017) Advancement and new perspectives of using formulated reactive amine blends for post-combustion carbon dioxide (CO2) capture technologies. Petroleum. KeAi Communications Co., pp. 10–36. https://doi.org/10.1016/j.petlm.2016.11.002

Olabi AG et al (2022) Assessment of the pre-combustion carbon capture contribution into sustainable development goals SDGs using novel indicators. Renew Sustain Energy Rev 153. https://doi.org/10.1016/j.rser.2021.111710.

Ouyang L et al (2021) Nitrogen-doped porous carbon materials derived from graphene oxide/melamine resin composites for co2 adsorption. Molecules 26(17). https://doi.org/10.3390/molecules26175293

Pandey S et al (2021) Graphene nanosheets derived from plastic waste for the application of DSSCs and supercapacitors. Sci Rep 11(1). https://doi.org/10.1038/s41598-021-83483-8

Policicchio A et al (2014) Cu-BTC/aminated graphite oxide composites as high-efficiency Co2 capture media. ACS Appl Mater Interfaces 6(1):101–108. https://doi.org/10.1021/am404952z

Politakos N et al (2020) Reduced graphene oxide/polymer monolithic materials for selective CO2 capture. Polymers 12(4). https://doi.org/10.3390/POLYM12040936

Qiu X et al (2022) A stable and easily regenerable solid amine adsorbent derived from a polyethylenimine-impregnated dialdehyde-cellulose/graphene-oxide composite. New J Chem 46(15):6956–6965. https://doi.org/10.1039/d2nj00530a

Ramar V, Balraj A (2022) Critical review on carbon-based nanomaterial for carbon capture: technical challenges, opportunities, and future perspectives. Energy and Fuels. Am Chem Soc 13479–13505. https://doi.org/10.1021/acs.energyfuels.2c02585

Raymundo-Piñero E et al (2005) KOH and NaOH activation mechanisms of multiwalled carbon nanotubes with different structural organisation. Carbon 43(4):786–795. https://doi.org/10.1016/j.carbon.2004.11.005

Rosmi MS et al (2016) Synthesis of uniform monolayer graphene on resolidified copper from waste chicken fat by low pressure chemical vapor deposition. Mater Res Bull 83:573–580. https://doi.org/10.1016/j.materresbull.2016.07.010

Roy I et al (2016) Synthesis and characterization of graphene from waste dry cell battery for electronic applications. RSC Adv 6(13):10557–10564. https://doi.org/10.1039/c5ra21112c

Ruan G et al (2011) Growth of graphene from food, insects, and waste. ACS Nano 5(9):7601–7607. https://doi.org/10.1021/nn202625c

Salih E, Ayesh AI (2020) CO, CO2, and SO2 detection based on functionalized graphene nanoribbons: first principles study. Physica E 123(May):114220. https://doi.org/10.1016/j.physe.2020.114220

Scholes CA et al (2020) Membrane gas-solvent contactor pilot plant trials for post-combustion CO2 capture. Sep Purif Technol 237. https://doi.org/10.1016/j.seppur.2019.116470

Seema H et al (2014) Highly selective CO2 capture by S-doped microporous carbon materials. Carbon 66:320–326. https://doi.org/10.1016/j.carbon.2013.09.006

Seo HK et al (2015) Value-added synthesis of graphene: recycling industrial carbon waste into electrodes for high-performance electronic devices. Sci Rep 5(November):1–10. https://doi.org/10.1038/srep16710

Seo DH et al (2017) Single-step ambient-air synthesis of graphene from renewable precursors as electrochemical genosensor. Nat Commun 8. https://doi.org/10.1038/ncomms14217

Shah J et al (2018) Plasma synthesis of graphene from mango peel. ACS Omega 3(1):455–463. https://doi.org/10.1021/acsomega.7b01825

Shams SS et al (2015) Synthesis of graphene from biomass: a green chemistry approach. Mater Lett 161:476–479. https://doi.org/10.1016/j.matlet.2015.09.022

Shen Y, Lua AC (2013) A facile method for the large-scale continuous synthesis of graphene sheets using a novel catalyst. Sci Rep 3. https://doi.org/10.1038/srep03037

Silvestre SL et al (2022) Cork derived laser-induced graphene for sustainable green electronics. Flex Print Electron 7(3). https://doi.org/10.1088/2058-8585/ac8e7b

Singh PK et al (2023) Green synthesis and characterizations of citric acid-functionalized graphene oxide via electrochemical method: in situ surface modification using citric acid. Int J Mod Phys B [Preprint]. https://doi.org/10.1142/S0217979223501953

Stankovic B et al (2022) Comparison of experimental and quantum chemical studies of the effect of different functionalities of graphene oxide/polymer composites onto selective CO2 capture IKERBASQUE. Basque Found Sci. https://doi.org/10.21203/rs.3.rs-1522884/v1

Sun C et al (2015) Application of nanoporous graphene membranes in natural gas processing: molecular simulations of CH4/CO2, CH4/H2S and CH4/N2 separation. Chem Eng Sci 138:616–621. https://doi.org/10.1016/j.ces.2015.08.049

Sun PZ et al (2021) Exponentially selective molecular sieving through angstrom pores. Nat Commun 12(1). https://doi.org/10.1038/s41467-021-27347-9

Tamilselvi R et al (2020) Graphene oxide – based supercapacitors from agricultural wastes: a step to mass production of highly efficient electrodes for electrical transportation systems. Renew Energy 151:731–739. https://doi.org/10.1016/j.renene.2019.11.072

Tarcan R et al (2020) Reduced graphene oxide today. J Mater Chem C. Royal Soc Chem 1198–1224. https://doi.org/10.1039/c9tc04916a

Udhaya Sankar G, Ganesa Moorthy C, RajKumar G (2018) Synthesizing graphene from waste mosquito repellent graphite rod by using electrochemical exfoliation for battery/supercapacitor applications. Energy Sources, Part A: Recover, Utilization Environ Eff 40(10):1209–1214. https://doi.org/10.1080/15567036.2018.1476609

Viculis LM, Mack JJ, Kaner RB (2003) A chemical route to carbon nanoscrolls. Science 299(5611):1361. https://doi.org/10.1126/science.1078842

Wang Z et al (2016) Large-scale and controllable synthesis of graphene quantum dots from rice husk biomass: a comprehensive utilization strategy. ACS Appl Mater Interfaces 8(2):1434–1439. https://doi.org/10.1021/acsami.5b10660

Wang M et al (2020) Penta-graphene as a promising controllable CO2 capture and separation material in an electric field. Appl Surf Sci 502. https://doi.org/10.1016/j.apsusc.2019.144067

Wang Z et al (2021) Space-confined carbonization strategy for synthesis of carbon nanosheets from glucose and coal tar pitch for high-performance lithium-ion batteries. Appl Surf Sci 547. https://doi.org/10.1016/j.apsusc.2021.149228

Wei K et al (2022) Recent advances in CO2 capture and reduction. Nanoscale 14(33):11869–11891. https://doi.org/10.1039/d2nr02894h

Wilberforce T et al (2019) Outlook of carbon capture technology and challenges. Sci Total Environ 657:56–72. https://doi.org/10.1016/j.scitotenv.2018.11.424

Wu H et al (2019) Numerical simulation of oxy-fuel combustion characteristics in a 200 MWe coal-fired boiler. Greenh Gases: Sci Technol 9(2):276–286. https://doi.org/10.1002/ghg.1844

Wu K et al (2022) Graphene oxide-doped stearate-intercalated layered double oxide nanocomposites as high-performance CO2 adsorbents. Sep Purif Technol 288. https://doi.org/10.1016/j.seppur.2022.120686

Xia K et al (2014) Hierarchical porous graphene-based carbons prepared by carbon dioxide activation and their gas adsorption properties. Int J Hydrogen Energy 39(21):11047–11054. https://doi.org/10.1016/j.ijhydene.2014.05.059

Yan Y et al (2021) Synthesis of graphene oxide and graphene quantum dots from miscanthus via ultrasound-assisted mechano-chemical cracking method. Ultrason Sonochem 73. https://doi.org/10.1016/j.ultsonch.2021.105519

Yaqoob AA et al (2021) Self-assembled oil palm biomass-derived modified graphene oxide anode: an efficient medium for energy transportation and bioremediating Cd (II) via microbial fuel cells. Arab J Chem 14(5). https://doi.org/10.1016/j.arabjc.2021.103121

Zhang S et al (2022) A density functional theory study on the adsorption reaction mechanism of double CO2 on the surface of graphene defects. J Mol Model 28(5):1–11. https://doi.org/10.1007/s00894-022-05105-y

Zhao H, Zhao TS (2013) Graphene sheets fabricated from disposable paper cups as a catalyst support material for fuel cells. J Mater Chem A 1(2):183–187. https://doi.org/10.1039/c2ta00018k

Zhao Y et al (2012) Preparation and characterization of aminated graphite oxide for CO 2 capture. Appl Surf Sci 258(10):4301–4307. https://doi.org/10.1016/j.apsusc.2011.12.085

Zhao Y et al (2014) Insight into the mechanism of CO2 adsorption on Cu-BTC and its composites with graphite oxide or aminated graphite oxide. Chem Eng J 239:399–407. https://doi.org/10.1016/j.cej.2013.11.037

Zhao H et al (2022) Insights into the performance of hybrid graphene oxide/MOFs for CO2 capture at process conditions by molecular simulations. Chem Eng J 449. https://doi.org/10.1016/j.cej.2022.137884

Zhu X et al (2022) Recent advances in direct air capture by adsorption. Chem Soc Rev 51(15):6574–6651. https://doi.org/10.1039/d1cs00970b

Zhu Y et al (2011) Carbon-based supercapacitors produced by activation of graphene. https://doi.org/10.1126/science.1200770

Publisher's Note Springer Nature remains neutral with regard to jurisdictional claims in published maps and institutional affiliations.

Springer Nature or its licensor (e.g. a society or other partner) holds exclusive rights to this article under a publishing agreement with the author(s) or other rightsholder(s); author self-archiving of the accepted manuscript version of this article is solely governed by the terms of such publishing agreement and applicable law.